Published in final edited form as:

Matter. 2024 April 03; 7(4): 1533–1557. doi:10.1016/j.matt.2024.01.023.

Tension in the ranks: Cooperative cell contractions drive force-dependent collagen assembly in human fibroblast culture

Alexandra A. Silverman[1], **Jason D. Olszewski**[1], **Seyed Mohammad Siadat**[1], **Jeffrey W. Ruberti**[1,2,*]

[1]Department of Bioengineering, Northeastern University, Boston, MA, USA

[2]Lead contact

SUMMARY

Currently, there is no mechanistic model that fully explains the initial synthesis and organization of durable animal structure. As a result, our understanding of extracellular matrix (ECM) development and pathologies (e.g., persistent fibrosis) remains limited. Here, we identify and characterize cell-generated mechanical strains that direct the assembly of the ECM. Cell kinematics comprise cooperative retrograde “pulls” that organize and precipitate biopolymer structure along lines of tension. High-resolution optical microscopy revealed five unique classes of retrograde “pulls” that result in the production of filaments. Live-cell confocal imaging confirmed that retrograde pulls can directly cause the formation of fibronectin filaments that then colocalize with collagen aggregates exported from the cell, producing persistent elongated structures aligned with the direction of the tension. The findings suggest a new model for initial durable structure formation in animals. The results have important implications for ECM development and growth and life-threatening pathologies of the ECM, such as fibrosis.

Graphical Abstract

*Correspondence: j.ruberti@northeastern.edu.

AUTHOR CONTRIBUTIONS

Conceptualization, J.W.R.; methodology, A.A.S., J.D.O., S.M.S., and J.W.R.; investigation, A.A.S. and J.W.R.; Data collection, A.A.S. and J.D.O.; formal analysis, A.A.S., J.D.O., S.M.S., and J.W.R.; resources, J.W.R.; data curation, A.A.S. and J.D.O.; writing – original draft, A.A.S., S.M.S., and J.W.R.; writing – review & editing, A.A.S., J.D.O., S.M.S., and J.W.R.; visualization, A.A.S. and J.W.R.; supervision, A.A.S., S.M.S., and J.W.R.; project administration, J.W.R.; funding acquisition, J.W.R.

SUPPLEMENTAL INFORMATION

Supplemental information can be found online at https://doi.org/10.1016/j.matt.2024.01.023.

DECLARATION OF INTERESTS

The authors declare no competing interests.

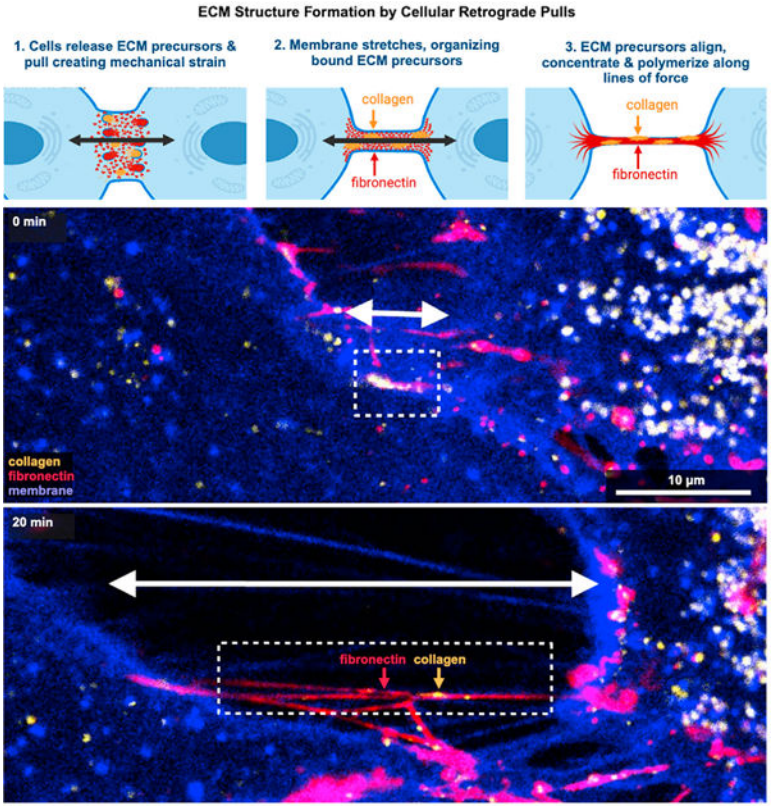

The precise mechanisms that control and form animal structure remain unclear. Using an *in vitro* model of corneal development, we directly observed the detailed motion of human cells as they began making the incipient fine filaments destined to be woven into the durable structure that becomes a tissue. To produce these initial filaments, we observed that the cells must contract toward themselves and away from each other to generate mechanical tension, which then produces structure in the path of force.

INTRODUCTION

The function of load-bearing (e.g., tendon) and other highly specialized tissues (e.g., cornea) is critically dependent on the precise placement and retention of structural polymers directly in the path of mechanical force. In vertebrates, fibroblastic cells work with their associated molecular secretome to efficiently generate a fully continuous, mechanically competent, polymeric extracellular matrix (ECM) orders of magnitude larger than themselves. The precise mechanisms driving ECM formation remain obscure because it is difficult to observe morphogenesis at high enough temporal and spatial resolution to determine the fate of structural molecules as they move from synthesis to secretion and incorporation into the developing durable tissue.[1] Thus, most knowledge has been gained indirectly through destructive, static, high-spatial-resolution electron microscopy[2–7] or lower-spatial-resolution optical microscopy.[5,6] While dynamic live-imaging studies, precisely focused on ECM deposition, have the potential to reveal the mechanism of matrix formation, there have been very few of them,[8,9] and they have not examined the correct temporal and spatial window

to reveal the incipient mechanism of deposition. We are thus left with little data capable of explaining structural causality with respect to the morphogenesis of organized connective tissue.

It is known that the genesis of durable structure (e.g., collagen fibrils) depends on the formation of adhesion complexes on the cell surface,[10] the polymerization of actin filaments,[11] the presence of fibronectin (FN),[12] and the ability of cells to provide a force or to "pull."[13–15] In 2016, we demonstrated that extensional strain alone could drive collagen fibrillogenesis in a cell-free solution of collagen molecules.[16] In that study, extensional strain rates on the order of 0.3 s^{-1} caused the flow-induced crystallization (FIC) of collagen molecules, a concept well known in polymer physics.[17,18] Flow-induced aggregation (FIA) of numerous important biomolecules (such as FN and tau protein) has also been demonstrated.[19–23] We suggested that fibroblasts might be capable of initiating assembly of ECM materials by pulling receptor-laden cell processes through an extracellular macromolecular milieu containing crowded ECM components, including collagen, FN, and hyaluronan (HA).[16] FN is a particularly important player as it flow aggregates easily[20] and can "catalyze" collagen fibril formation, lowering the barriers to FIC.[21]

Using an *in vitro* model of corneal stromal development,[5,9,24] we investigated whether and how human fibroblasts use mechanical tension to polymerize ECM structures. This model permits live, direct observation of primary human corneal fibroblast (PHCF) cell-matrix interactions. Using differential interference contrast (DIC) microscopy, we can take images at relatively high spatial (structures down to ~30 nm are detectable)[25] and temporal (seconds between images) resolution. Here, we combine our PHCF ECM morphogenesis model with live DIC and confirmatory live confocal fluorescence imaging to examine ECM deposition during the critical window where durable matrix is initially formed.

RESULTS AND DISCUSSION

Cell kinematics

Live DIC microscopy revealed that filaments form via multiple types of cell contractions—Using live DIC microscopy to visualize PHCF growth to confluency on days 1–4, we observed that PHCFs generate "filaments" via rapid cellular retrograde contractions that we term "pulls." These pulls were productive in that they "caused" the formation of persistent filaments, which we believe to be a form of retraction fiber.[26] However, we could not easily fit these structures into a single class of retraction fiber; thus, we refer to them here only as filaments with the understanding that they are produced via a retrograde contraction or pull.

We recorded and categorized pulling events that led to filament formation based on the morphology of the pull. We identified five distinct types of pulls. (1) Flat cell process (CP) pull (Figure 1A): originating from transparent lamellipodium-like projections at the cell edges, these pulls can occur either between two cells or from a single cell anchored to a glass surface. They result in nearly parallel filaments that align with the axis of the pull and are perpendicular to the cell border. (2) Thick CP pull (Figure 1B): characterized by wide "foot pads" at the end of CPs, these pulls often form the entire trailing edge of a cell

and exhibit a “bubbling” behavior, releasing vesicles into the extracellular space. (3) Thin CP pull (Figure 1C): notably thinner than thick CPs ($p < 0.05$), these pulls can occur at any angle relative to the cell’s long axis and do not usually constitute the entire trailing edge of the cell. About 50% of these pulls exhibit minor bubbling, either within the CP itself or at the base of the forming filament. (4) Ultrafine CP pull (Figure 1D): created by the thinnest and longest CPs, these are reminiscent of tunneling nanotubes (TNTs). TNTs are actin-rich nanotubular structures stretched between cells above their substrate and facilitate the intercellular transfer of organelles, membrane components, and cytoplasmic molecules.[27,28] In our videos, ultrafine CPs always extend between two cells, and in 80% of cases, they contain gondola-like[29,30] vesicles (moving vesicles in TNTs that are bigger than the diameter of the respective TNT itself; a reference to a gondola aerial lift) transported within the pull. (5) Cell surface pull (Figure 1E): resulting from rapid contraction of the cell body or the rapid separation of two adjacent cells, these filaments appear to originate from nucleation points on the cell surface.

The number of filaments generated during each pull was recorded, and the most prominent filament was selected for calculating extensional strain rate and pull velocity. The data from this analysis can be found in Table S1. Figure 1 and Video S1 provide representative examples for each category of pull, along with their corresponding velocity and extensional strain rate plots. Additional examples for each type of pull can be seen in Figure S1 and Video S2.

During the growth phase to confluency on glass substrates, we observed diverse filament formation patterns. Specifically, some filaments formed between a cell and its underlying glass substrate, while other filaments formed between two cells. In cases where two cells were involved, the pulls were further categorized as either symmetric (both cells contracted in what appeared to be a coordinated event) or asymmetric (only one cell contracted). When single-celled contractions occurred, the cell pulled against the culture dish surface and deposited filaments directly on the glass. Figure S2 and Video S3 show representative still images and videos for the subcategories of symmetric, asymmetric, and single-celled pulling.

Pulls generate extensional strain rates capable of forming collagen fibrils via FIC—Generally, pulls exhibited an initial slow contraction, then a sharp rise to maximum velocity, followed by a sharp decrease as the retrograde pulling event ended (Figure 2A). An analysis of 130 pulling events across days 1–4 and various pull types (Figure 2B) revealed an average maximum pull velocity of 0.80 ± 0.93 μm/s ($n = 130$), which is over 20 times faster than the average mid-stage retraction fiber speed (0.038 μm/s)[26] and over 250 times faster than the migration speed of our PHCFs on glass (0.003 μm/s). Figure 2C provides a breakdown of maximum pull velocities for each specific pull type. Taken together, these results suggest that cell motility was *not* the primary objective of the pulling events.

The average maximum extensional strain rate was $0.23 \pm 0.44\ s^{-1}$ ($n = 130$), and the highest extensional strain rates created by flat CP, thick CP, and thin CP pulls exceeded $1\ s^{-1}$ (Figure 2D). These strain rates are within the range ($0.3\ s^{-1}$) capable of forming collagen fibrils

via FIC in a cell-free system.[16] However, all pulls analyzed were “productive” in that they produced observable filaments, even at the lowest extensional strain rates of 0.01 s^{-1}.

Notable pulling event observations—Through extensive observation using live DIC microscopy, we identified several key phenomena that could offer insights into the underlying mechanisms of filament formation (Figure 3; Video S4).

Vesicle dynamics suggest active material transfer during filament formation.: Previous live-imaging data have shown that cells aggregate surface “bubbles” (vesicles) where filaments form.[31,32] Here, bubbles were often observed at the site of filament formation immediately prior to the pull, and in some cases, they would shrink or disappear following the contraction, suggesting that their contents may have been ejected or unspooled during the pulling event (refer to Figure 3A and the first pull in Video S4).

A reeling-in mechanism amplifies the filament extensional strain rate.: In many pulling events, the filaments were not only extended by the retraction of the CP that created them, but they were also “reeled in” toward the cell body at the same time[26] (see Figure 3B and the second pull in Video S4). This likely makes the actual extensional strain rate of the filament higher than could be calculated by simply measuring the change in length of the filament.

Changes in cell surface curvature during pulling events.: Prior to some pulling event, the curvature at the base of the forming filament appears to be relatively open (refer to Figure 3C and the third pull in Video S4). However, as the pull unfolds, we observe a pronounced increase in cell surface curvature. This observed change is reminiscent of the “necking region” previously documented by Paten et al.[16]

Orthogonal pulling in PHCFs: Evidence of cellular bi-directionality influencing tissue structure.: In this culture system[5] and in their natural state, PHCFs produce nearly orthogonal sheets of collagen. Interestingly, we observed numerous cases where the same cell would pull in one direction (typically along its principal axis) and then immediately pull at a different angle (often orthogonally) to the previous pull (see Figure 3D and the fourth pull in Video S4). This suggests that there may be some cellular internal bi-directionality or bi-polarization that is instrumental in the ultimate orthogonal organization of the tissue produced.

Molecular crowding has no effect on pull kinematics.: Molecular crowding of corneal fibroblasts can convert secreted procollagen to telocollagen (i.e., activated for assembly)[33] and drastically enhance the rate of matrix deposition.[34,35] We conducted this experiment with and without Ficoll as a molecular crowding agent. While the addition of Ficoll to the culture system resulted in thicker constructs at 2 weeks (20.38 ± 6.36 μm vs. 12.95 ± 1.87 μm, $p = 0.03$), we did not observe significant differences in the types of pulls, maximum pull velocities, or maximum extensional strain rates during the initial 4-day observation period in the crowded versus uncrowded experiments and, thus, pooled the data.

Molecular composition and dynamics

Filaments comprising thin cellular extensions engage with developing FN and collagen matrix—Figure 4 shows the progression of the cell culture by DIC and live-cell fluorescence microscopy over the 4 days of observation and at a later time point on day 7. While the cell density of the culture increases each day, it is clear from the fluorescence images that filaments containing both collagen and FN form at the earliest time points, with both biopolymers generally increasing in quantity over time. During days 1–2, FN is observed on specific regions of the cell membrane, with punctate aggregates of exported collagen colocalizing with FN membrane filaments. By days 3–4, FN strands extend between cells, and collagen adopts a more linear arrangement, suggesting the formation of collagen filaments. By day 7, continuous collagen filaments separate from FN membrane structures to create stand-alone structures, which we anticipate will become “durable” over time.

Lower-temporal-resolution (every 5 min) confocal imaging of the pulling events shows that the majority of fast pulling events formed thin, undecorated membrane extensions (Figure 5). We further found that exported collagen and FN aggregates could bind to and stretch with some of these membrane extensions. Even at the earliest culture time points, collagen and FN were present on some filaments, and collagen was clearly colocalized, translocated, and stretched with the FN. These observations suggest that exported “mutable” aggregates of collagen are captured and reformed into linear structures by association with the FN in our system.

Biopolymer flow aggregation and co-association during pulling events—Figure 6 and Video S5 show a clear example of flow aggregation and FN/collagen co-association during a pulling event. In the video, we see the exportation of punctate collagen aggregates to the cell surface, followed by a pulling event that creates an array of continuous FN filaments that colocalize with the exported collagen, pulling it along with the stretching FN. The FN/collagen association is consistent across our observation period, with nearly all observed forming collagen filaments colocalized with extending FN filaments.

If the filaments were indeed being stretched during the pulling event, as opposed to being pulled pre-formed out of a cell compartment, this could function to concentrate any bound precursor biopolymers and extend them in the direction of load, likely aiding in polymerization. To investigate this, we assessed the thickness change of a subset of pulls (n = 9) using DIC microscopy.[36] Figure S3 shows thinning of filaments during the contraction. However, we cannot state with any certainty that *all* filaments thinned during the pulling events; indeed, there appear to be cases where some filaments are formed from vesicular contents directly (see Figure 3A) and likely do not thin proportional to their extension with deposition.

Our findings are consistent with those of Young et al.[4] and Bueno et al.[37] who both observed that thin cell extensions associate with the forming collagen matrix. Young et al. termed these matrix-forming structures “keratopodia.” These cell extensions are likely important drivers of early matrix assembly and are possibly critical to fibrotic tissue formation, where the cells are highly contractile. To determine whether the same kind of pulling kinematics

and resultant filament composition occur in a different species, we examined the behavior of rat embryonic fibroblasts under the same conditions and observed similar filament formation and kinematic behavior (Figure S4).

Post-formation mutability of collagen filaments guided by FN and mechanical strain—When formed, short collagen filaments are not static but can undergo further stretching and re-organization through interactions with FN/cell membrane extensions and subsequent pulling events. Figure 7 and Video S6 demonstrate that short collagen filaments can bind to FN, elongate in tandem with FN/membrane filaments, and align according to the most recent pulls. The video reveals a collagen filament (indicated by the lower dotted circle) detaching from FN at the 80-min mark. Upon release of tension, it extends its tip toward another FN filament, becoming longer and again stretching in the direction of the pull by the end of the video. Notably, the upper dotted circle highlights two collagen filaments at the 85-min mark that are bound to the same FN filament; these filaments stretch, and one subsequently fuses to itself laterally. These observations suggest that both lateral and longitudinal growth of collagen fibrils could be facilitated by molecular crowding (via adhesion to FN/membrane filaments) and mechanical strain (induced by pulling events).

Mechanisms of collagen scavenging and potential recycling—Video S6 illustrates how a collagen filament stretches farther when it binds to a prominent FN filament during a new pulling event. Conversely, Figure 8 and Video S7 show that, when a collagen filament fails to bind to a strong FN filament, it is scavenged by the cell. In this sequence, a cell approaches the collagen (Figure 8A), binds to it (Figure 8B), and pulls it inward (Figure 8C). The collagen then disengages from the small FN aggregate to its left (Figure 8D), tension is released (Figure 8E), and, ultimately, the collagen is scavenged (Figure 8F). It is possible that such scavenged collagen is recycled by the cell, as discussed previously.[38–43]

Spontaneous formation of collagen filaments without contraction events—In our culture system, we observed instances of “worm”-like collagen structures forming spontaneously between cells and the glass substrate without any associated contraction events (Figure 9; Video S8). These structures had an average length of 3.5 ± 1.0 μm (Figure S5) and were not under any tension. Their growth is likely the result of the enzymatic conversion of recently exported, punctate collagen aggregates. Three observers tracked the arc length of 10 such collagen worms as a function of time (Figure S5). The average growth rate was found to be 44 ± 17 nm/min over the monitoring period (44 ± 11 min), reaching an average peak growth rate of 101 ± 35 nm/min.

Pulls are discrete events that have characteristic kinematics capable of flow-induced protein aggregation or crystallization of biological polymers and form filaments between “anchor” points

Creating highly anisotropic arrays of collagen fibrils is critical for the mechanical function of tensile load-bearing (e.g., tendon) and specialized connective (e.g., the cornea) tissues. Fibroblast cells possess contractile machinery and polarization and thus have a ready mechanism to drive and control ECM organization: mechanical force. Mechanical forces are vectors (with direction and magnitude), operate over long distances, and are capable of

controlling connective tissue deposition.[44] Here we demonstrated that persistent filamentous structures form secondary to the act of a fibroblast, or portion thereof, pulling toward itself. The active elements involved in this process appear to include contracting cell surfaces (i.e., cell surface protrusions, lamellipodia, and CPs) and mechanosensitive biopolymers (FN and collagen), at least.

We label the events described in this study “pulls” to distinguish them from the normal movements of the cells. Pulls could involve single or multiple cells and different structures associated with each cell. A pull is a rapid kinematic event that has a clearly characteristic motion comprising three parts (Figure 2A): (1) slow initiation, stretching attachments, and building tension in the structures that connect the pulling cell to a collaborating cell or to the glass; (2) acceleration to a peak retraction velocity, well above average cell velocity, and attainment of peak extensional strain rate; and (3) sharp deceleration. Only one subset of pulls (ultrafine), which we believe were generating/extending TNTs, did not follow this pattern. TNTs are specialized cellular extensions that transport signals directly between cells.[45] They have been reported previously to be formed by myeloid cells in the adult mouse cornea,[46] fibroblast cells,[47] and other cell types[48] but not corneal fibroblast cells. While we did not intend to fully investigate TNTs in this study, for the first time we report formation of these structures between PHCFs and demonstrate how they can extend between cells via cellular contraction.

We did *not* observe any long, continuous filaments forming spontaneously in the culture system without an associated contraction event (note: short collagen worms did form in the confined space between the cells and the glass substrate; we suggest that this is artifactual due to the entrapment of the collagen between the cell and the glass), nor did we observe the pure extrusion of long filaments from cell invaginations or long filaments emerging from the cell surface in the absence of extensional mechanical assistance. All long forming filaments started and ended at fixed points, either on a cell surface, a CP, or on the glass. The initial connection between the surfaces that subsequently “separate” is thus an important mechanism to examine in detail. Our data further suggest that filaments are not being pre-formed within the cell and drawn out. In many cases, filaments grew to lengths longer than the cell body, providing further evidence that the filament was assembling, growing, or stretching as a direct result of the pull. Cooperation between cells is also likely critical for filament formation, and data on collagen fibril synthesis support this idea. Lu et al.[8] reported that individual collagen fibrils are formed by more than one cell when they used co-cultures of two different colored collagen-expressing cells.

Some pulls captured were of the highest velocities recorded in the literature for retrograde CP retraction.[49] For four of the pull categories, flat CP, thick CP, thin CP, and cell surface pulls, the maximum extensional strain rates were sufficient to cause collagen fibril formation via FIC based on the data of Paten et al.[16] and well above that needed for hybrid collagen/FN fiber formation via combined FIA/FIC, as shown by Paten et al.[21] However, the fact that filaments also formed at very low strain rates and under conditions of low precursor biopolymer concentration suggests that polymerization is assisted through binding to receptor-laden membrane extensions,[50] which collect, concentrate, and extend the precursor biopolymers to promote assembly. It is also important to note that most pulls do

not produce polymer assembly in our open, molecularly "uncrowded" culture system (even with the addition of Ficoll), which likely frustrates matrix production prior to confluency.

Proposed models of initial ECM filament formation—The long-standing model of collagen fibrillogenesis, initially proposed by Birk and Trelstad[7] and Trelstad and Hayashi[7,51] and further developed by Canty and Kadler[52] posits that cells directly generate fibrils within narrow plasma membrane channels and protrusions (fibripositors). Subsequently, based on the fibripositor model, collagen fibrils are discharged into the ECM to achieve tissue-specific organization. The fibripositor model, however, is not consistent with the strong evidence that hyaluronic acid,[53] FN,[12] actin filaments,[11] and integrins[10] are necessary for collagen fibrillogenesis (see Siadat et al.[1] for a more detailed discussion of the shortcoming of previous collagen fibrillogenesis models). Based on the data presented in the current study, we propose two possible models, along with relevant live-cell imaging examples, of ECM structure formation driven by cellular contractions (Figure 10; Video S9). The molecules included in our models are all known to assemble into fibers, with FN and collagen known to assemble under extensional strain.[16,20] Additionally, it is known that procollagen is exported to the surface in secretory granules[54] and that it (and its propeptidases) is potentially bound to FN to facilitate local activation.[55] While we did not stain for HA, we include it in the model as it is thought to assist in FN/collagen deposition,[56] and it is known that HA is synthesized by HAS-2[57] near the membrane. Because all filaments were formed by the mechanical separation of two structures, both of our models begin with the formation of an attachment between cells.

Model 1: CP/receptor-mediated FIA/FIC.: Figures 10A and 10B depict a stretching filament that has a long, thin cell surface extension at its center. In this model, the cellular retrograde pull stretches the cell membrane(s) into a long, thin filament replete with cell surface receptors that bind extracellular structural precursor biopolymers such as FN and collagen (synthesized previously or ejected concurrently from vesicles). The surface binding of precursor biopolymer molecules to an extending CP facilitates aggregation/crystallization in four important ways. (1) It reduces biopolymer motility, increasing the effective relaxation time. (2) As the CP thins and lengthens, it aligns the bound precursor biopolymers, extending them in the direction of load. (3) The radial contraction concentrates the biopolymers on the filament circumference. (4) The surface confinement prevents internal flows[16] that can disrupt formation of biopolymer structures. The combined effect produces physical conditions that, we hypothesize, promote the organized assembly/crystallization of ECM filaments.

All three of our candidate molecules are ligands for cell receptors found on corneal and other fibroblasts (HA-CD44,[58,59]; FN:a5b1,[60] and Col:a2b1[61]). Additionally, it has been demonstrated that monomeric collagen in solution rapidly homes to and incorporates with collagen fibrils under strain.[62] This model is also consistent with the co-alignment of corneal CPs ("keratopodia") with collagen arrays observed by Young et al.[4] and Bueno et al.[37]

Model 2: Pure FIA/FIC.: Figures 10C and 10D show filaments that are generated without a cell membrane extension at their core. The attachment point is formed so that biopolymer precursor molecules are positioned between the two surfaces. Upon retrograde pulling,

the dense polymer solution is stretched, rapidly "spooling" out of the vesicles to form filaments. (We believe that the first pull in Video S4 and Figure 3B, where the cell deposits matrix directly on glass purportedly from a vesicle, is a clear example of this model.) As the stretching progresses, the filament further thins and lengthens, and the dense molecular milieu outside of the cells (pre-synthesized or ejected concurrently from vesicles) may participate in the filament composition. In our system, we visualized FN from vesicles stretching to form thin filaments and visualized collagen aggregates colocalizing and stretching with these FN filaments.

Nearly all pulling events that generated ECM filaments followed model 1, where FN aggregates were stretched into a filament with the cell membrane at its core. Over time, the membrane core of these filaments would dissipate, and the filament would become re-associated with another cell surface and further stretched and organized (Figure 10E; Video S10). We also visualized collagen aggregates colocalizing and stretching along with FN to form durable structure that remained linear even when tension was removed (Figure 10F). We occasionally saw FN filaments form following model 2, where the filament spools out of a vesicle without a membrane core, but these filaments were very small and occurred during the initial days of culture. In both models, the durable filaments (collagen) separate from the FN after it facilitates their formation, completing the process of initial matrix morphogenesis (Figure S6).

There is strong evidence to support FN's role in collagen fibrillogenesis, where FN aids in the processing of procollagen by providing a scaffold for both procollagen and the C-propeptide proteinase bone morphogenetic protein 1 (BMP-1).[55] The meticulous experiments by Saunders and Schwarzbauer[55] suggest that, after cleavage, fibrillar collagen no longer requires association with FN. Their findings are consistent with our observation that collagen filaments eventually separate from FN after "maturation," as shown in Figure S6.

A note on the role of FN—The role of FN in the formation of durable collagen structure has been reconsidered recently.[63] We view FN as an assistive molecule, promoting the flow crystallization of collagen fibrils,[21] which do not flow assemble as readily as FN.[20] Thus FN, by binding collagen (i.e., increasing its relaxation time) and stretching it, thereby lowering its barrier to FIC,[35,64] is likely of great utility in producing durable structure in situations where the collagen cannot easily be preconcentrated, such as in wound healing, tissue remodeling, or open cell culture systems. However, under highly controlled conditions where collagen *can* be preconcentrated before pulling, such as in development, a substantial FN "assist" may not be as critical to promote collagen assembly.[63]

Collagen export to the ECM—Based on our imaging, there were two ways we observed collagen export to the ECM. In the first method, small, punctate, collagen-rich droplets appear on the surface of the cells. This collagen has two possible fates in our data: (1) it will bind in its amorphous form to FN that is close by and under tension, and (2) if there is no proximate FN, it can begin to polymerize into malleable "worms," which are then subject to binding and reformation along an FN filament. We did not detect membrane surrounding these emerging droplets (Figures 6 and 9). It is possible that the punctate collagen-rich

droplets were bound by membrane, but we did not observe the membrane due to the more prominent cell membrane in the background. Alternatively, it is possible that the collagen droplets are in liquid-liquid phase separations with the surrounding medium. In the second method of exportation, on which we have limited data, we observed large membrane-bound vesicles to undergo shrinkage (disruption) during a pull. Notably, collagen seems to emerge from the vesicle, binding to a proximate FN filament (Video S11).

Molecular interaction during and after fibril formation—The assembly mechanisms of fibrils differ between FN and collagen. FN undergoes assembly under tension[20] through force-driven conformational changes and unfolding of its cryptic modules.[65,66] In contrast, collagen flow crystallizes with an extensional strain, achieved by the co-alignment of molecules in an extensional flow.[16] The co-alignment changes the nature of the molecular interactions from 3D random collisions to lateral collisions of elongated molecules. The effect significantly reduces the activation energy for assembly (crystallization).[17,18,67] For a more in-depth exploration of force-driven assembly in biopolymers, please refer to a review by Siadat and Ruberti.[68]

After collagen fibril formation, the structural integrity is primarily maintained by hydrogen bonds, involving both intermolecular and intramolecular interactions.[69,70] Lysyl oxidase (LOX) cross-linking takes place subsequently, following the initial assembly of collagen fibrils. LOX catalyzes specific lysine and hydroxylysine residues in the N- and C-telopeptides, generating reactive aldehydes that form covalent intra- and inter-molecular cross-links. These divalent cross-links play a crucial role in stabilizing nascent fibrils and can eventually progress into mature trivalent cross-links by reacting with a third residue or another divalent cross-link. The abundance of trivalent cross-links increases during development as collagen fibers undergo hierarchical maturation.[71–73] Hence, we speculate that the observed collagen fibrils in our experiments are predominantly maintained by hydrogen bonds, and LOX-mediated cross-linking is likely to occur in a more mature ECM constructed by cells.

Implications of the observed behavior—There are a number of potential implications for ECM development, growth, maintenance, repair, and pathology if we cautiously extend the fundamental pulling behaviors observed in our model system to the *in vivo* cell-ECM relationship.

A new model of durable ECM formation: Mechanochemical force-structure causality.: The first implication is the potential discovery of a fundamental, proximal mechanism driving organized durable ECM production, which we posit to be mechanochemical in nature. In all cases, we observed that filaments were produced by pulling, and we describe this activity as mechanical causation of structure or, more formally, mechanochemical force-structure causality (MFSC).[68] Mechanical strain has been shown previously to *cause* structure formation for two of the three major structural biopolymers involved in the development of ECM: FN[65] and collagen.[16] In the case of FN, the deformation of the molecules opens a cryptic binding site to promote FN fiber assembly via FIA.[65] For collagen, extensional strain rates align molecules and accelerate assembly via FIC.[16] When FN and collagen are together, there is a synergistic effect, further lowering the

energy barrier to assembly.[21] The most important aspect of MFSC is that structure is formed directly in the path of the forces that create it, ostensibly to resist subsequent forces that propagate along the same direction. This is possibly why we first see cell and CP alignment with the eventual matrix that is formed in developing organized tissues.[4,7,74,75] Cells produce the initial structure along local lines of "pull," and then global-level tissue forces (i.e., muscle contractions, growth pressure increases) complete the structure formation, as described by Paten et al.[16] It has been shown that knocking out non-muscle myosin II disrupts initial collagen fibril formation,[14] abrogating muscle contractions cause tendon formation to fail,[76–79] and de-pressuring the ocular globe leads to impaired growth,[80] underscoring the importance of collaboration between global and cell-generated forces.

Prestress: Filament deposition under tension.: Tissues generally exhibit prestress, suggesting fibril deposition under tension,[81] If mechanical strains are required to cause the formation of structure, then the structures that are formed are going to be pre-strained by design. It is interesting to note that the seminal demonstration of engineered tissue formation was a collagen gel contracted by fibroblasts.[82]

Substrate effective stiffness: Soft vs. hard substrates.: Our cells were plated on glass, which is, in effect, infinitely stiff. Thus, cells can generate maximum forces and velocities, provided they were well anchored to the substrate. On very soft materials, fibroblasts cannot generate the same separation forces or speeds, limiting their ability to produce structure. Fibroblasts on soft tissues under load would experience an effectively higher resistance in the direction of force and strain, and therefore would likely be more effective at producing structure precisely where the loads are highest.

The structural organization kernel: Effect of cell polarization.: In our system, we used corneal stromal cells, which inherently produce orthogonal layers of parallel collagen fibrils. We found many examples of double pulls, where cells would pull in one direction and then follow that quickly by pulling in another direction, which was often close to orthogonal. We also visualized ECM filaments extending in an "L shape" at the cell surface, with one end extending along the cell surface and the other perpendicular to the cell surface, bridging the gap between two adjacent cells (Figure S7). Electron micrographs[7] and reconstructions[4] of developing chick cornea show that the same cell has collagen fibrils extending in two directions from the cell body. Therefore, multiple pulling directions could be fundamental to the ultimate organization of the tissue being constructed.

Fibrosis, wound healing, and tissue engineering.: Nearly 45% of all deaths worldwide are related to some form of fibrosis.[83] It is well known that increased contractile machinery is present in myofibroblasts and that the transformation of local fibroblasts to myofibroblasts is a marker of fibrosis.[84] The increased muscularity of myofibroblasts could cause the formation of pathogenic structure through MFSC, provided there are available precursor biopolymers. Further, as structure is produced and stiffens, the effectiveness of each pull likely increases, leading to more accumulation of ECM in a positive feedback loop. When we understand the incipient mechanisms of fibrosis, there are opportunities to control or

reverse it. As a corollary, wound healing and engineering of ECM tissues could be enhanced through the harnessing of MFSC principles.

Study limitations

First, there is limited physiological relevance of early cultures on glass. Our experimental model is a human primary cell culture system that is known to produce orthogonal arrays of collagen, in an arrangement similar to the native cornea stroma, over a period of weeks. Early on, when there is minimal molecular crowding to prevent molecules from diffusing away, the cells cannot produce extensive matrix because collagen is lost to the medium prior to conversion by propeptidases.[85] Thus, we are observing the actions of a frustrated matrix production culture system working with a limited supply of precursor biopolymer molecules. Additionally, these cells behave more like myofibroblasts than fibroblasts in early culture, so the timing of this model could be more representative of healing than development. However, prior to confluence, we can better observe and quantify their behavior with high-resolution DIC. Furthermore, because of filaments' extreme fragility during fixation and immunohistochemistry (IHC) staining (Figure S8), live cell stains were necessary to identify components associated with the forming filaments. Last, there are potentially interfering effects of FN and other components in the system due to the presence of bovine serum in the medium.

Conclusion

Our observations, performed at high spatial and temporal resolution, support the principal hypothesis that structures (filaments) are formed preferentially "along the lines of local mechanical strain." More succinctly, we directly observed mechanical causation of biological structure at the cellular-length scale. These data suggest that local pulling leads to durable structure formation in an *in vitro* model of developing ECM. The nature of the pulling profile indicates that pulling events are separate and distinct from those that provide cell motility or apply tension in general. Tying mechanical force and the resulting strain rates directly to biopolymer structure formation via FIA and FIC could lead to a clearer, functional understanding of the cell-matrix interplay during development, growth, and pathological changes of connective tissues (e.g., fibrosis). There are rather important implications associated with the proposed MFSC model. However, on a more philosophical note, if millions of micron-scale, cooperative cell contractions cause the formation of tiny polymeric strings that integrate to form our load-bearing structure, then we could be, quite literally, "pulled" into existence.

EXPERIMENTAL PROCEDURES

Resource availability

Lead contact—Further information and resource requests should be sent to the lead contact, Jeffrey W. Ruberti (j.ruberti@northeastern.edu).

Materials availability—No new unique materials were produced by this investigation.

Data and code availability—No data or code are available for request.

Cell isolation and culture

PHCFs were isolated from 74-year-old or 67-year-old human donor corneas (obtained through the National Disease Research Interchange) following the procedure established by Bueno et al.[37] Briefly, donor corneas were gently scraped of their epithelium and endothelium to ensure that only stromal cells were isolated. Then, the corneas were cut into 2 × 2 mm pieces and cleaned by soaking in 1× Gibco phosphate-buffered saline (PBS) (Thermo Fisher Scientific, 10–010–023) containing 1% HyClone penicillin-streptomycin 100× solution (Thermo Fisher Scientific, SV30010) and 0.1% amphotericin B (250 μg/mL) solution (Sigma-Aldrich, 1397–89–3).

Each explant was adhered to the center of a 6-well culture plate (Corning, 3516), and PHCFs were cultured using the reagents and techniques established by Siadat et al.[86] Complete PHCF medium, comprising Corning DMEM with L-glutamine and 4.5 g/L glucose without sodium pyruvate (Thermo Fisher Scientific, MT10017CV), 1% penicillin-streptomycin, 0.1% amphotericin B, and 10% Corning regular fetal bovine serum (Thermo Fisher Scientific, MT35010CV), was gently added to the well. Cells were incubated at 37°C with 5% CO_2. A half-medium exchange was performed every 3–5 days until the PHCFs migrated off the explant. When confluent, the explants were discarded, and PHCFs were expanded and frozen for future use.

Rat embryonic fibroblasts (ATCC, Rat2 CRL-1764) were cultured with complete rat medium, comprising DMEM with L-glutamine, glucose, and sodium pyruvate (ATCC, 30–2002), 1% penicillin-streptomycin, 0.1% amphotericin B, and 10% Corning regular fetal bovine serum, under the same conditions as PHCFs.

Live-cell DIC imaging

PHCF cells from the 74-year-old donor were seeded at passage 3 on uncoated, 170-μm-thick, glass-bottomed, temperature-controlled culture dishes (Bioptechs, 04200417B) at a concentration of 10,000 cells/cm^2. On day 1, a full medium exchange was performed, and CO_2-infused, complete medium containing 0.5 mM L-ascorbic acid (Sigma-Aldrich, A4544) was added to stabilize the collagen produced by the culture. For half of the samples, 37.5 mg/mL Ficoll 70 (Sigma-Aldrich, F2878) and 25 mg/mL Ficoll 400 (Sigma-Aldrich, F8016) were added to the medium to increase the molecular crowding of ECM proteins. 6 PHCF samples treated with only ascorbic acid and 6 PHCF samples treated with ascorbic acid, Ficoll 70, and Ficoll 400 were assessed.

After the medium was exchanged, the cells were incubated for 3 h and then imaged with a coverglass lid (Bioptechs, 4200312) using a Nikon Eclipse TE2000-E inverted microscope. A 60× Nikon CFI Apochromat total internal reflection fluorescence (TIRF) oil objective and Photometrics CoolSNAP EZ charge-coupled device (CCD) camera were used to take high-resolution DIC photos every 5 s for 1 h. The Nikon Perfect Focus system was utilized to ensure that the sample remained in focus during imaging. To keep the sample at 37°C, an objective heater (Bioptechs, 150819), an objective heater controller (Bioptechs, 150803), a microscope stage adapter (Bioptechs, 04202602), and a culture dish temperature controller

(Bioptechs, 0420–04–03) were used. All samples were imaged at approximately the same location to ensure a consistent distribution of cells.

After imaging the sample, it was placed back in the incubator to be subsequently imaged on days 2, 3, and 4. On days 2 and 4, no medium exchange was performed prior to imaging. On day 3, a full medium exchange was performed 3 h prior to imaging using CO_2-infused complete medium containing either only 0.5 mM L-ascorbic acid or 0.5 mM L-ascorbic acid, 37.5 mg/mL Ficoll 70, and 25 mg/mL Ficoll 400.

Rat2 cells were imaged only on day 3 following the same methods as for PHCF cells. Complete rat medium containing 0.5 mM L-ascorbic acid, 37.5 mg/mL Ficoll 70, and 25 mg/mL Ficoll 400 was used.

Assessing cell culture thickness

After DIC imaging on day 4, PHCF samples were grown until day 14 with full medium exchanges every 2–3 days using complete medium with consistent concentrations of either only L-ascorbic acid or L-ascorbic acid, Ficoll 70, and Ficoll 400. On day 14, cell construct thickness was assessed by using the Nikon inverted microscope with the 60× oil objective and DIC to perform a Z scan in center, north, south, east, and west locations in each cell culture. Multiple locations were used due to heterogeneity in the cell culture; these locations were averaged to obtain a mean thickness for each cell construct.

DIC time-lapse analysis

Time-lapse videos were analyzed frame by frame using Fiji.[87] For each identified pull, the length of the most prominent persistent filament was measured over time, and the following equations were used to analyze the pulling events:

$$\text{PHCF pull velocity: } v_n = \frac{L_n - L_{n-1}}{t_n - t_{n-1}}$$

$$\text{PHCF pull extensional strain rate: } \dot{\varepsilon}_n = \frac{(L_n - L_{n-1})/L_{n-1}}{t_n - t_{n-1}}$$

where L_n is the length of the persistent filament in frame n, L_{n-1} is the length of the persistent filament in the previous frame $(n-1)$, t_n is the time in frame n, and t_{n-1} is the time at the previous frame. Though our microscope was set to take photos every 5 s, this timing was not always precise, and images were taken approximately every 4–6 s. For our analysis, we used the exact time points exported from our data.

A total of 130 pulling events were analyzed individually by three authors to obtain 3 measurements for length, 3 measurements for velocity, and 3 measurements for extensional strain rate for each pull at each time point. These values were averaged to obtain a mean length, velocity, and extensional strain rate for each pull at each time point. The maximum velocity and extensional strain rate for each pulling event was used to compare events.

Pulling events were subsequently categorized into five pull types based on pull morphology. For pulling events that created multiple persistent filaments, we recorded the total number of filaments created and their maximum length and then analyzed the most prominent and visible filament. The length of the contracting CP and its average thickness were recorded. To determine CP thickness, measurements were taken at 5 locations along the process and then averaged. For each pulling event, it was noted whether the CP contained a bubbling footpad and whether the event occurred between two cells or one cell and the glass surface of the culture dish.

DIC-edge intensity shift (DIC-EIS) analysis for estimating filament diameter changes

Filament diameter change was estimated from DIC images based on a method that measures collagen fibril diameter.[36] Only filaments that stayed in focus during the entire pulling event were analyzed. Briefly, DIC images were uploaded into MATLAB. A rectangular region of interest was defined along the middle section of each filament. DIC-EIS was calculated as the average difference between the maximum and minimum intensities across each filament.

Live-cell confocal imaging

CNA35-EGFP, a collagen binding protein with green fluorescent protein, was prepared following the protocol established by Aper et al.[88] Briefly, single *E. coli* colonies with the pET28a-EGFP-CNA35 gene (Addgene, plasmid 61603) were cultured in LB (Lysogeny broth) medium, and protein expression was induced with 0.5 mM isopropyl β-D-1-thiogalactopyranoside (Sigma-Aldrich, I1284). Bacterial pellets were resuspended in Bugbuster (Sigma-Aldrich, 70584–3) containing 1 μL/mL benzonase (Thermo Fisher Scientific, 70–746–3). Protein was purified via Ni^{2+} affinity chromatography using the N-terminal 6xHis-tag.

FN stain was prepared by mixing 100 μL Alexa Fluor 594 anti-FN antibody (Abcam, ab275336) with 0.3 mL glycerol (Thermo Fisher Scientific, G33), 0.01 g bovine serum albumin (Sigma-Aldrich, A8654), and 0.6 mL PBS (Thermo Fisher Scientific, AAJ67670AP) to create a stock solution of 50 μg/mL antibody that was stored at −20°C until use.

For each sample, (1) nucleus-membrane and (2) collagen-FN staining solutions were prepared with complete medium containing 0.5 mM L-ascorbic acid, 37.5 mg/mL Ficoll 70, and 25 mg/mL Ficoll 400. Nucleus-membrane staining medium was supplemented with 2 drops/mL of NucBlue (Thermo Fisher Scientific, R37605) and 1 μL/mL CellBrite Steady Membrane Dye (Biotium, 30105-T and 30108-T). Initially, CellBrite Steady Membrane Dye 405 nm was used, but it was replaced with CellBrite Steady Membrane Dye 650 nm due to phototoxicity. Collagen-FN staining medium was supplemented with 20 μL/mL CNA35-EGFP and 15 μL/mL FN stain.

Cells from the 67-year-old donor were cultured on Bioptechs culture dishes with complete medium containing 0.5 mM L-ascorbic acid, 37.5 mg/mL Ficoll 70, and 25 mg/mL Ficoll 400 as described previously. Prior to imaging, a full medium exchange was performed, 1 mL of nucleus-membrane staining medium was added, and cells were incubated for 30 min at 37°C and 5% CO_2. Then, another full medium exchange was performed, 1 mL

of collagen-FN staining medium was added, and cells were incubated for at least 30 min at 37°C and 5% CO_2. This collagen-FN staining medium was kept in the dish during all confocal imaging.

Cells were imaged on a Carl Zeiss LSM 880 confocal laser-scanning microscope using a 63× oil objective with controlled incubation settings of 37°C, 5% CO_2, and humidity. Cells were imaged using 405-nm, 488-nm, 561-nm, and 640-nm laser lines with a pixel dwell time of either 0.55 μs or 1.1 μs. The laser intensity, pinhole size, and gain were optimized to decrease photobleaching while enabling visualization of fine filaments. Live-cell confocal time-lapse images were taken every 5 min. Z stacks and tile scans were also performed. After imaging, cells were discarded.

Video creation

Files were imported into Fiji[87] as an image sequence and cropped, rotated, and adjusted to have increased contrast and better showcase the pulling event. All image modifications (i.e., rotations, contrast enhancement, etc.) were minimal and applied to the entire image. The scale bar and time stamp were also added in Fiji.[87] Our time stamp was set to increase in increments of either 5 s (for DIC imaging) or 5 min (for confocal imaging). Photoshop and BioRender were utilized to create video annotations, and iMovie was used to assemble and edit the videos.

Supplementary Material

Refer to Web version on PubMed Central for supplementary material.

ACKNOWLEDGMENTS

This work was supported by funding from NIH/NEI 1R21EY029167 and NIH/NEI R01EY034124 and two Northeastern University Undergraduate Research and Fellowships PEAK Experiences Awards. Images were created with BioRender. We thank the Institute for Chemical Imaging of Living Systems (RRID: SCR_022681) at Northeastern University for consultation and instrument support.

REFERENCES

1. Siadat SM, Zamboulis DE, Thorpe CT, Ruberti JW, and Connizzo BK (2021). Tendon extracellular matrix assembly, maintenance and dysregulation throughout life. In Progress in Heritable Soft Connective Tissue Diseases, pp. 45–103.
2. Birk DE, Zycband EI, Winkelmann DA, and Trelstad RL (1989). Collagen fibrillogenesis in situ: fibril segments are intermediates in matrix assembly. Proc. Natl. Acad. Sci. USA 86, 4549–4553. 10.1073/pnas.86.12.4549. [PubMed: 2734306]
3. Birk DE, Zycband EI, Woodruff S, Winkelmann DA, and Trelstad RL (1997). Collagen fibrillogenesis in situ: fibril segments become long fibrils as the developing tendon matures. Dev Dyn 208, 291–298. 10.1002/(SICI)1097-0177(199703)208:3<291::AID-AJA1>3.0.CO;2-D. [PubMed: 9056634]
4. Young RD, Knupp C, Pinali C, Png KMY, Ralphs JR, Bushby AJ, Starborg T, Kadler KE, and Quantock AJ (2014). Three-dimensional aspects of matrix assembly by cells in the developing cornea. Proc. Natl. Acad. Sci. USA 111, 687–692. 10.1073/pnas.1313561110. [PubMed: 24385584]
5. Guo X, Hutcheon AEK, Melotti SA, Zieske JD, Trinkaus-Randall V, and Ruberti JW (2007). Morphologic characterization of organized extracellular matrix deposition by ascorbic acid-stimulated human corneal fibroblasts. Invest. Ophthalmol. Vis. Sci 48, 4050–4060. 10.1167/iovs.06-1216. [PubMed: 17724187]

6. Saeidi N, Guo X, Hutcheon AEK, Sander EA, Bale SS, Melotti SA, Zieske JD, Trinkaus-Randall V, and Ruberti JW (2012). Disorganized collagen scaffold interferes with fibroblast mediated deposition of organized extracellular matrix in vitro. Biotechnol. Bioeng 109, 2683–2698. 10.1002/bit.24533. [PubMed: 22528405]
7. Birk DE, and Trelstad RL (1984). Extracellular compartments in matrix morphogenesis: collagen fibril, bundle, and lamellar formation by corneal fibroblasts. J. Cell Biol 99, 2024–2033. [PubMed: 6542105]
8. Lu Y, Kamel-El Sayed SA, Wang K, Tiede-Lewis LM, Grillo MA, Veno PA, Dusevich V, Phillips CL, Bonewald LF, and Dallas SL (2018). Live Imaging of Type I Collagen Assembly Dynamics in Osteoblasts Stably Expressing GFP and mCherry-Tagged Collagen Constructs. J. Bone Miner. Res 33, 1166–1182. 10.1002/jbmr.3409. [PubMed: 29461659]
9. Zareian R, Susilo ME, Paten JA, McLean JP, Hollmann J, Karamichos D, Messer CS, Tambe DT, Saeidi N, Zieske JD, and Ruberti JW (2016). Human Corneal Fibroblast Pattern Evolution and Matrix Synthesis on Mechanically Biased Substrates. Tissue Eng 22, 1204–1217. 10.1089/ten.TEA.2016.0164.
10. Li S, Van Den Diepstraten C, D'souza SJ, Chan BMC, and Pickering JG (2003). Vascular smooth muscle cells orchestrate the assembly of type I collagen via a2b1 integrin, RhoA, and fibronectin polymerization. Am. J. Pathol 163, 1045–1056. [PubMed: 12937145]
11. Johnson C, and Galis ZS (2003). Quantitative assessment of collagen assembly by live cells. Journal of Biomedical Materials Research Part A: An Official Journal of The Society for Biomaterials. In The Japanese Society for Biomaterials, and the Australian Society for Biomaterials and the Korean Society for Biomaterials, 67The Japanese Society for Biomaterials, and the Australian Society for Biomaterials and the Korean Society for Biomaterials, pp. 775–784.
12. Sottile J, and Hocking DC (2002). Fibronectin polymerization regulates the composition and stability of extracellular matrix fibrils and cell-matrix adhesions. Mol. Biol. Cell 13, 3546–3559. [PubMed: 12388756]
13. Canty EG, Starborg T, Lu Y, Humphries SM, Holmes DF, Meadows RS, Huffman A, O'Toole ET, and Kadler KE (2006). Actin filaments are required for fibripositor-mediated collagen fibril alignment in tendon. J. Biol. Chem 281, 38592–38598. [PubMed: 17020878]
14. Kalson NS, Starborg T, Lu Y, Mironov A, Humphries SM, Holmes DF, and Kadler KE (2013). Nonmuscle myosin II powered transport of newly formed collagen fibrils at the plasma membrane. Proc. Natl. Acad. Sci. USA 110, E4743–E4752. 10.1073/pnas.1314348110. [PubMed: 24248360]
15. Kapacee Z, Richardson SH, Lu Y, Starborg T, Holmes DF, Baar K, and Kadler KE (2008). Tension is required for fibripositor formation. Matrix Biol 27, 371–375. 10.1016/j.matbio.2007.11.006. [PubMed: 18262777]
16. Paten JA, Siadat SM, Susilo ME, Ismail EN, Stoner JL, Rothstein JP, and Ruberti JW (2016). Flow-Induced Crystallization of Collagen: A Potentially Critical Mechanism in Early Tissue Formation. ACS Nano 10, 5027–5040. 10.1021/acsnano.5b07756. [PubMed: 27070851]
17. Rao I, and Rajagopal K (2001). A study of strain-induced crystallization of polymers. Int. J. Solid Struct 38, 1149–1167.
18. Keller A (1997). Flow-Induced Orientation and Structure Formation. In Proc, Polymers. Materials science and technology: a comprehensive treatment, 18, pp. 189–268.
19. Hosseini H, Rangchian A, Prins ML, Giza CC, Ruberti JW, and Kavehpour HP (2020). Probing Flow-Induced Biomolecular Interactions With Micro-Extensional Rheology: Tau Protein Aggregation. J. Biomech. Eng 142, 034501. [PubMed: 34043752]
20. Ejim OS, Blunn GW, and Brown RA (1993). Production of artificial-orientated mats and strands from plasma fibronectin: a morphological study. Biomaterials 14, 743–748. [PubMed: 8218723]
21. Paten JA, Martin CL, Wanis JT, Siadat SM, Figueroa-Navedo AM, Ruberti JW, and Deravi LF (2019). Molecular Interactions between Collagen and Fibronectin: A Reciprocal Relationship that Regulates De Novo Fibrillogenesis. Chem-Us 5, 2126–2145. 10.1016/j.chempr.2019.05.011.
22. Smith ML, Gourdon D, Little WC, Kubow KE, Eguiluz RA, Luna-Morris S, and Vogel V (2007). Force-induced unfolding of fibronectin in the extracellular matrix of living cells. PLoS Biol 5, e268. 10.1371/journal.pbio.0050268. [PubMed: 17914904]

23. Dobson J, Kumar A, Willis LF, Tuma R, Higazi DR, Turner R, Lowe DC, Ashcroft AE, Radford SE, Kapur N, and Brockwell DJ (2017). Inducing protein aggregation by extensional flow. Proc. Natl. Acad. Sci. USA 114, 4673–4678. [PubMed: 28416674]
24. Ren R, Hutcheon AEK, Guo XQ, Saeidi N, Melotti SA, Ruberti JW, Zieske JD, and Trinkaus-Randall V (2008). Human primary corneal fibroblasts synthesize and deposit proteoglycans in long-term 3-D cultures. Dev. Dynam 237, 2705–2715.
25. Allen RD, Allen NS, and Travis JL (1981). Video-enhanced contrast, differential interference contrast (AVEC-DIC) microscopy: A new method capable of analyzing microtubule-related motility in the reticulopodial network of Allogromia laticollaris. Cell Motil 1, 291–302. [PubMed: 7348605]
26. Cramer LP, and Mitchison TJ (1997). Investigation of the mechanism of retraction of the cell margin and rearward flow of nodules during mitotic cell rounding. Mol. Biol. Cell 8, 109–119. 10.1091/mbc.8.1.109. [PubMed: 9017599]
27. Gerdes H-H, Bukoreshtliev NV, and Barroso JFV (2007). Tunneling nanotubes: a new route for the exchange of components between animal cells. FEBS Lett 581, 2194–2201. [PubMed: 17433307]
28. Matejka N, and Reindl J (2019). Perspectives of cellular communication through tunneling nanotubes in cancer cells and the connection to radiation effects. Radiat. Oncol 14, 218. [PubMed: 31796110]
29. Drab M, Stopar D, Kralj-Iglič V, and Iglič A (2019). Inception mechanisms of tunneling nanotubes. Cells 8, 626. [PubMed: 31234435]
30. Hurtig J, Chiu DT, and Önfelt B (2010). Intercellular nanotubes: insights from imaging studies and beyond. Wiley Interdiscip. Rev. Nanomed. Nanobiotechnol 2, 260–276. [PubMed: 20166114]
31. Stearns ML (1940). Studies on the development of connective tissue in transparent chambers in the rabbit's ear. II. Am. J. Anat 67, 55–97.
32. Stearns ML (1940). Studies on the development of connective tissue in transparent chambers in the rabbit's ear. I. Am. J. Anat 66, 133–176.
33. Bateman JF, Cole WG, Pillow JJ, and Ramshaw JA (1986). Induction of procollagen processing in fibroblast cultures by neutral polymers. J. Biol. Chem 261, 4198–4203. [PubMed: 2869039]
34. Kumar P, Satyam A, Fan X, Collin E, Rochev Y, Rodriguez BJ, Gorelov A, Dillon S, Joshi L, Raghunath M, et al. (2015). Macromolecularly crowded in vitro microenvironments accelerate the production of extracellular matrix-rich supramolecular assemblies. Sci. Rep 5, 8729. 10.1038/srep08729. [PubMed: 25736020]
35. Graham J, Raghunath M, and Vogel V (2019). Fibrillar fibronectin plays a key role as nucleator of collagen I polymerization during macromolecular crowding-enhanced matrix assembly. Biomater. Sci 7, 4519–4535. 10.1039/c9bm00868c. [PubMed: 31436263]
36. Siadat SM, Silverman AA, DiMarzio CA, and Ruberti JW (2021). Measuring Collagen Fibril Diameter with Differential Interference Contrast Microscopy. J. Struct. Biol 213, 107697. [PubMed: 33545351]
37. Bueno EM, Saeidi N, Melotti S, and Ruberti JW (2009). Effect of serum and insulin modulation on the organization and morphology of matrix synthesized by bovine corneal stromal cells. Tissue Eng 15, 3559–3573. 10.1089/ten.TEA.2008.0404.
38. ten Cate AR (1972). Morphological studies of fibrocytes in connective tissue undergoing rapid remodelling. J. Anat 112, 401–414. [PubMed: 4629130]
39. Cate AR, and Deporter DA (1975). The degradative role of the fibroblast in the remodelling and turnover of collagen in soft connective tissue. Anat. Rec 182, 1–13. [PubMed: 168793]
40. Ten Cate AR, and Deporter DA (1974). The role of the fibroblast in collagen turnover in the functioning periodontal ligament of the mouse. Arch. Oral Biol 19, 339–340. [PubMed: 12692920]
41. Ten Cate AR, and Freeman E (1974). Collagen remodelling by fibroblasts in wound repair. Preliminary observations. Anat. Rec 179, 543–546. [PubMed: 4842940]
42. Deporter DA, and ten Cate AR (1973). Fine structural localization of acid and alkaline phosphatase in collagen-containing vesicles of fibroblasts. J. Anat 114, 457–461. [PubMed: 4716142]
43. Cate AR, and Syrbu S (1974). A relationship between alkaline phosphatase activity and the phagocytosis and degradation of collagen by the fibroblast. J. Anat 117, 351–359. [PubMed: 4461726]

44. Bhole AP, Flynn BP, Liles M, Saeidi N, Dimarzio CA, and Ruberti JW (2009). Mechanical strain enhances survivability of collagen micronetworks in the presence of collagenase: implications for load-bearing matrix growth and stability. Philos. Trans. A Math. Phys. Eng. Sci 367, 3339–3362. 10.1098/rsta.2009.0093. [PubMed: 19657003]
45. Dupont M, Souriant S, Lugo-Villarino G, Maridonneau-Parini I, and Vérollet C (2018). Tunneling Nanotubes: Intimate Communication between Myeloid Cells. Front. Immunol 9, 43. 10.3389/fimmu.2018.00043. [PubMed: 29422895]
46. Seyed-Razavi Y, Hickey MJ, Kuffová L, McMenamin PG, and Chinnery HR (2013). Membrane nanotubes in myeloid cells in the adult mouse cornea represent a novel mode of immune cell interaction. Immunol. Cell Biol 91, 89–95. [PubMed: 23146944]
47. Panasiuk M, Rychłowski M, Derewońko N, and Bieńkowska-Szewczyk K (2018). Tunneling nanotubes as a novel route of cell-to-cell spread of herpesviruses. J. Virol 92, e00090–18. 10.1128/jvi.00090-00018. [PubMed: 29491165]
48. Sisakhtnezhad S, and Khosravi L (2015). Emerging physiological and pathological implications of tunneling nanotubes formation between cells. Eur. J. Cell Biol 94, 429–443. [PubMed: 26164368]
49. Kress H, Stelzer EHK, Holzer D, Buss F, Griffiths G, and Rohrbach A (2007). Filopodia act as phagocytic tentacles and pull with discrete steps and a load-dependent velocity. Proc. Natl. Acad. Sci. USA 104, 11633–11638. 10.1073/pnas.0702449104. [PubMed: 17620618]
50. Lee SY, Choi SH, Lee MS, Kurmashev A, Lee HN, Ko YG, Lee K, Jeong S, Seong J, Kang JH, and Kim H (2021). Retraction fibers produced by fibronectin-integrin alpha5beta1 interaction promote motility of brain tumor cells. Faseb. J 35, e21906. 10.1096/fj.202100452RR. [PubMed: 34490940]
51. Trelstad RL, and Hayashi K (1979). Tendon collagen fibrillogenesis: intracellular subassemblies and cell surface changes associated with fibril growth. Dev. Biol 71, 228–242. [PubMed: 499658]
52. Canty EG, and Kadler KE (2005). Procollagen trafficking, processing and fibrillogenesis. J. Cell Sci 118, 1341–1353. [PubMed: 15788652]
53. Goldberg B, and Green H (1964). An analysis of collagen secretion by established mouse fibroblast lines. J. Cell Biol 22, 227–258. [PubMed: 14195613]
54. Marchi F, and Leblond CP (1983). Collagen biogenesis and assembly into fibrils as shown by ultrastructural and 3H-proline radioautographic studies on the fibroblasts of the rat food pad. Am. J. Anat 168, 167–197. 10.1002/aja.1001680206. [PubMed: 6650434]
55. Saunders JT, and Schwarzbauer JE (2019). Fibronectin matrix as a scaffold for procollagen proteinase binding and collagen processing. Mol. Biol. Cell 30, 2218–2226. 10.1091/mbc.e19-03-0140. [PubMed: 31242089]
56. Evanko SP, Potter-Perigo S, Petty LJ, Workman GA, and Wight TN (2015). Hyaluronan Controls the Deposition of Fibronectin and Collagen and Modulates TGF-beta1 Induction of Lung Myofibroblasts. Matrix Biol 42, 74–92. 10.1016/j.matbio.2014.12.001. [PubMed: 25549589]
57. Guo N, Li X, Mann MM, Funderburgh ML, Du Y, and Funderburgh JL (2010). Hyaluronan Synthesis Mediates the Fibrotic Response of Keratocytes to Transforming Growth Factor β. J. Biol. Chem 285, 32012–32019. 10.1074/jbc.m110.127183. [PubMed: 20685654]
58. Zhu SN, Nölle B, and Duncker G (1997). Expression of adhesion molecule CD44 on human corneas. Br. J. Ophthalmol 81, 80–84. 10.1136/bjo.81.1.80. [PubMed: 9135415]
59. Al-Rekabi Z, Fura AM, Juhlin I, Yassin A, Popowics TE, and Sniadecki NJ (2019). Hyaluronan-CD44 interactions mediate contractility and migration in periodontal ligament cells. Cell Adhes. Migrat 13, 138–150. 10.1080/19336918.2019.1568140.
60. Masur SK, Cheung JK, and Antohi S (1993). Identification of integrins in cultured corneal fibroblasts and in isolated keratocytes. Invest. Ophthalmol. Vis. Sci 34, 2690–2698. [PubMed: 8344791]
61. Stepp MA (2006). Corneal integrins and their functions. Exp. Eye Res 83, 3–15. 10.1016/j.exer.2006.01.010. [PubMed: 16580666]
62. Siadat SM (2020). On the Mechanobiology of Collagen Growth and Remodelling. Ph.D (Northeastern University).
63. Musiime M, Chang J, Hansen U, Kadler KE, Zeltz C, and Gullberg D (2021). Collagen Assembly at the Cell Surface: Dogmas Revisited. Cells 10, 662. [PubMed: 33809734]

64. Kadler KE, Hill A, and Canty-Laird EG (2008). Collagen fibrillogenesis: fibronectin, integrins, and minor collagens as organizers and nucleators. Curr. Opin. Cell Biol 20, 495–501. 10.1016/j.ceb.2008.06.008. [PubMed: 18640274]
65. Baneyx G, and Vogel V (1999). Self-assembly of fibronectin into fibrillar networks underneath dipalmitoyl phosphatidylcholine monolayers: Role of lipid matrix and tensile forces. Proc. Natl. Acad. Sci. USA 96, 12518–12523. 10.1073/pnas.96.22.12518. [PubMed: 10535954]
66. Singh P, Carraher C, and Schwarzbauer JE (2010). Assembly of fibronectin extracellular matrix. Annu. Rev. Cell Dev. Biol 26, 397–419. [PubMed: 20690820]
67. Mackley M, and Keller A (1975). Flow induced polymer chain extension and its relation to fibrous crystallization. Phil. Trans. Roy. Soc. Lond. Math. Phys. Sci 278, 29–66.
68. Siadat SM, and Ruberti JW (2023). Mechanochemistry of collagen. Acta Biomater 163, 50–62. 10.1016/j.actbio.2023.01.025. [PubMed: 36669548]
69. Bansal M, Ramakrishnan C, and Ramachandran G (1975). Stabilization of the Collagen Structure by Hydroxyproline Residues (Springer), pp. 152–164.
70. Némethy G, and Scheraga HA (1986). Stabilization of collagen fibrils by hydroxyproline. Biochemistry 25, 3184–3188. [PubMed: 3730354]
71. Eyre DR, Paz MA, and Gallop PM (1984). Cross-linking in collagen and elastin. Annu. Rev. Biochem 53, 717–748. [PubMed: 6148038]
72. Yamauchi M, and Sricholpech M (2012). Lysine post-translational modifications of collagen. Essays Biochem 52, 113–133. [PubMed: 22708567]
73. Bates ME, Troop L, Brown ME, and Puetzer JL (2023). Temporal application of lysyl oxidase during hierarchical collagen fiber formation differentially effects tissue mechanics. Acta Biomater 160, 98–111. [PubMed: 36822485]
74. Hayes AJ, Isaacs MD, Hughes C, Caterson B, and Ralphs JR (2011). Collagen fibrillogenesis in the development of the annulus fibrosus of the intervertebral disc. Eur. Cell. Mater 22, 226–241. 10.22203/ecm.v022a18. [PubMed: 22048900]
75. Birk DE, and Trelstad RL (1986). Extracellular compartments in tendon morphogenesis: collagen fibril, bundle, and macroaggregate formation. J. Cell Biol 103, 231–240. 10.1083/jcb.103.1.231. [PubMed: 3722266]
76. Peterson BE, Rolfe RA, Kunselman A, Murphy P, and Szczesny SE (2021). Mechanical Stimulation via Muscle Activity is Necessary for the Maturation of Tendon Multiscale Mechanics during Embryonic Development. Front Cell Dev Biol 9, 725563. 10.3389/fcell.2021.725563. [PubMed: 34540841]
77. Schwartz AG, Lipner JH, Pasteris JD, Genin GM, and Thomopoulos S (2013). Muscle loading is necessary for the formation of a functional tendon enthesis. Bone 55, 44–51. 10.1016/j.bone.2013.03.010. [PubMed: 23542869]
78. Subramanian A, Kanzaki LF, Galloway JL, and Schilling TF (2018). Mechanical force regulates tendon extracellular matrix organization and tenocyte morphogenesis through TGFbeta signaling. Elife 7, e38069. 10.7554/elife.38069. [PubMed: 30475205]
79. Thomopoulos S, Kim H-M, Rothermich SY, Biederstadt C, Das R, and Galatz LM (2007). Decreased muscle loading delays maturation of the tendon enthesis during postnatal development. J. Orthop. Res 25, 1154–1163. 10.1002/jor.20418. [PubMed: 17506506]
80. Coulombre AJ (1957). The Role of Intraocular Pressure in the Development of the Chick. AMA. Arch. Ophthalmol 57, 250–253. 10.1001/archopht.1957.00930050260015. [PubMed: 13393895]
81. Ambrosi D, Ben Amar M, Cyron CJ, Desimone A, Goriely A, Humphrey JD, and Kuhl E (2019). Growth and remodelling of living tissues: perspectives, challenges and opportunities. J. R. Soc. Interface 16, 20190233. 10.1098/rsif.2019.0233. [PubMed: 31431183]
82. Bell E, Ivarsson B, and Merrill C (1979). Production of a tissue-like structure by contraction of collagen lattices by human fibroblasts of different proliferative potential in vitro. Proc. Natl. Acad. Sci. USA 76, 1274–1278. [PubMed: 286310]
83. Murtha LA, Schuliga MJ, Mabotuwana NS, Hardy SA, Waters DW, Burgess JK, Knight DA, and Boyle AJ (2017). The Processes and Mechanisms of Cardiac and Pulmonary Fibrosis. Front. Physiol 8, 777. 10.3389/fphys.2017.00777. [PubMed: 29075197]

84. Layton TB, Williams L, McCann F, Zhang M, Fritzsche M, Colin-York H, Cabrita M, Ng MTH, Feldmann M, Sansom SN, et al. (2020). Cellular census of human fibrosis defines functionally distinct stromal cell types and states. Nat. Commun 11, 2768. 10.1038/s41467-020-16264-y. [PubMed: 32488016]

85. Church RL (1980). Procollagen and collagen produced by normal bovine corneal stroma fibroblasts in cell culture. Invest. Ophthalmol. Vis. Sci 19, 192–202. [PubMed: 7351353]

86. Siadat SM, Silverman AA, Susilo ME, Paten JA, DiMarzio CA, and Ruberti JW (2022). Development of Fluorescently Labeled, Functional Type I Collagen Molecules. Macromol. Biosci 22, 2100144.

87. Schindelin J, Arganda-Carreras I, Frise E, Kaynig V, Longair M, Pietzsch T, Preibisch S, Rueden C, Saalfeld S, Schmid B, et al. (2012). Fiji: an open-source platform for biological-image analysis. Nat. Methods 9, 676–682. 10.1038/nmeth.2019. [PubMed: 22743772]

88. Aper SJA, van Spreeuwel ACC, van Turnhout MC, van der Linden AJ, Pieters PA, van der Zon NLL, de la Rambelje SL, Bouten CVC, and Merkx M (2014). Colorful protein-based fluorescent probes for collagen imaging. PLoS One 9, e114983. 10.1371/journal.pone.0114983. [PubMed: 25490719]

Highlights

- The kinematics of fibroblast motion were quantified
- Five unique classes of retrograde pulls by fibroblasts were identified
- Pulls resulted in formation of fibrillar fibronectin and collagen in ECM
- A new model for initial durable structure formation in animals is proposed

PROGRESS AND POTENTIAL

The work presented here has the potential to dramatically alter our understanding of durable structure (load-bearing tissue) formation in vertebrate animals. The current models of tissue production do not generally contemplate mechanical tension as a direct catalyst for the assembly of structural biopolymers (e.g., collagen) that will then resist the very forces that create them. If tension can induce the formation of structure directly in the path of the force that creates it, then there are large-scale implications across multiple research and therapeutic domains, from developmental biology to wound healing to orthopedic tissue repair and enhancement. The investigation formally introduces mechanochemistry to matrix formation at the cellular level and suggests that animals could be quite literally “pulled” into existence.

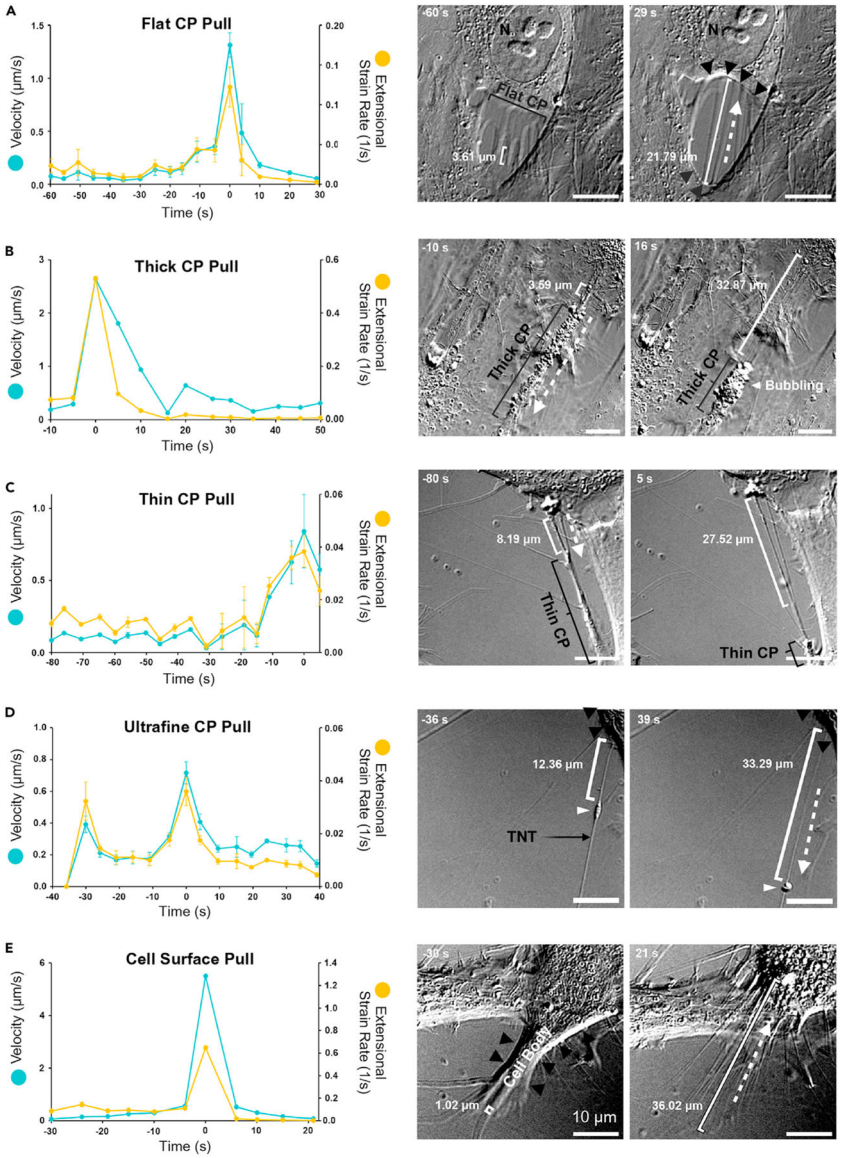

Figure 1. Classification of five types of retrograde pulls with corresponding kinematics

(A–E) Representative PHCF DIC live-cell images for each identified pull type. Initial and final time points are shown on the right, while the corresponding velocity and extensional strain rate plots are displayed on the left. Kinematics data are represented as mean ± standard deviation, based on observations from three independent analysts. Filaments under tension during pulling events are denoted in white brackets. Scale bars represent 10 μm. Dashed white arrows show the direction of pulls. Black arrowheads show the cell borders involved in the pulls. N, nucleus. Images are snapshots taken at initial and final timepoints in Video S1.

(A) Flat CP pulls are formed by transparent, lamellipodium-like projections at the cell edge, resulting in nearly parallel filaments that align with the direction of pulling and are perpendicular to the cellular border.

(B) Thick CP pulls are characterized by a broad “foot pad” at the end of the cellular extension, capable of generating multiple filaments. Notably, 90% of thick CPs display vesicle “bubbling” at their foot pads. They generally align with the cell’s long axis and often constitute the entire trailing edge of a cell.

(C) Thin CP pulls are distinguished by their significantly reduced width compared with thick CPs ($p < 0.05$). They can orient at any angle relative to the cell’s long axis and usually do not constitute the entire trailing edge of the cell. Approximately half exhibit minor vesicle bubbling, either by the CP itself or by the collaborating cell at the base of the forming filament.

(D) Ultrafine CP pulls are generated by the thinnest and longest cellular extensions, resembling TNTs. Most contain gondola-shaped vesicles (indicated by white arrowheads) that move along with the pulling force.

(E) Cell surface pulls occur when a large portion of the cell body contracts quickly or when two adjacent, parallel cells rapidly separate. Filaments in this category appear to nucleate directly from the cell surface, in contrast to those in flat CP pulls, which are formed by stretching flat lamellipodia.

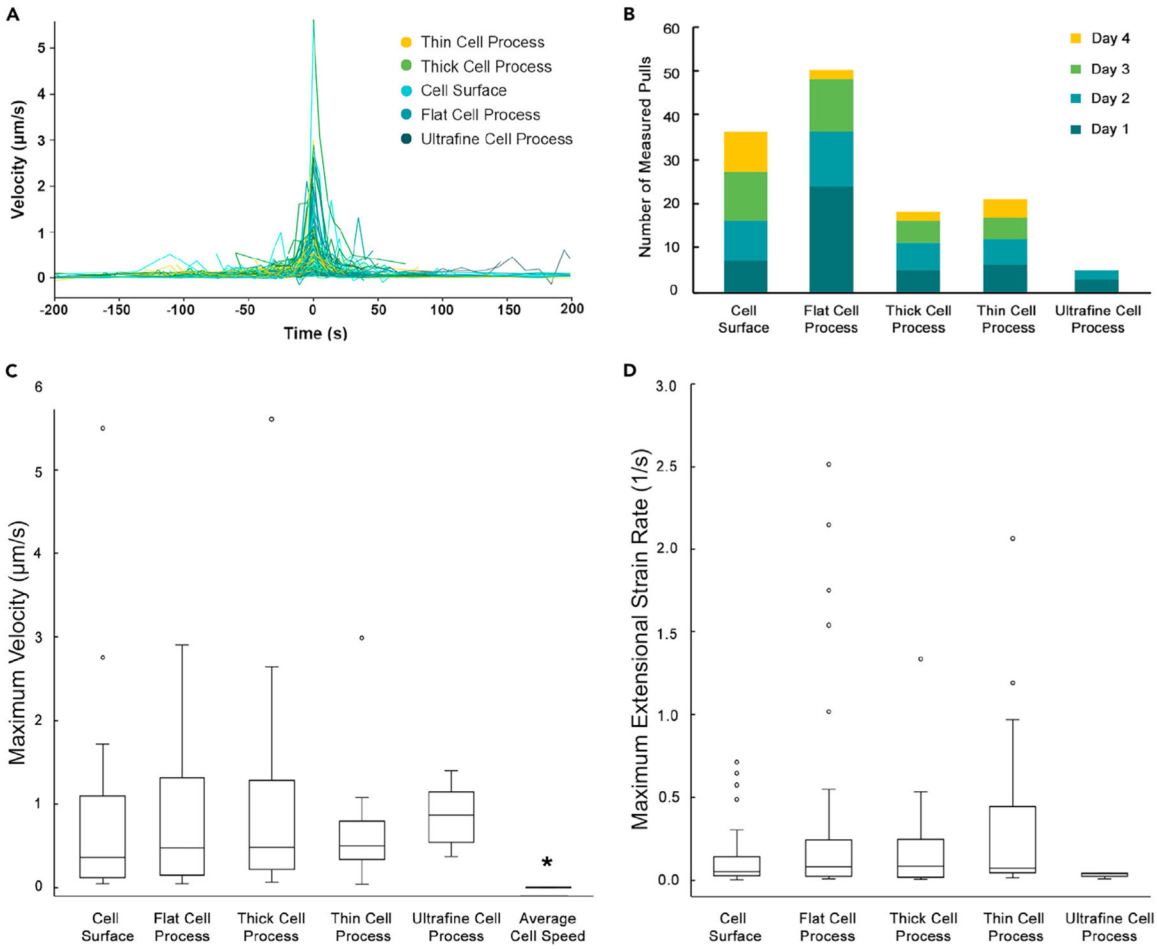

Figure 2. Kinematic analysis of retrograde pulling events

(A) Velocity profiles. The graph standardizes 130 assessed retrograde pulling events with maximum velocity set at time 0. Initially, pulling elements stretch their connecting structures to build tension, resulting in a slow onset of motion (left side of plot). As more contractile elements engage and some structures yield to the applied load, pulling events accelerate to their peak retraction velocity and extensional strain rate (center of plot). Eventually, the pull velocity sharply declines as the local cellular motion arrests (right side of plot).

(B) Temporal distribution. This plot shows the distribution of assessed pulling events across days 1–4, categorized by pull type.

(C) Maximum pull velocity. Shown is a boxplot comparing the maximum pull velocity for each identified pull type. The average PHCF migration speed was found to be significantly slower ($p < 0.01$) than the average maximum contraction velocity across all pull types.

(D) Maximum extensional strain rate. Shown is a boxplot depicting the maximum extensional strain rate observed for each pull type.

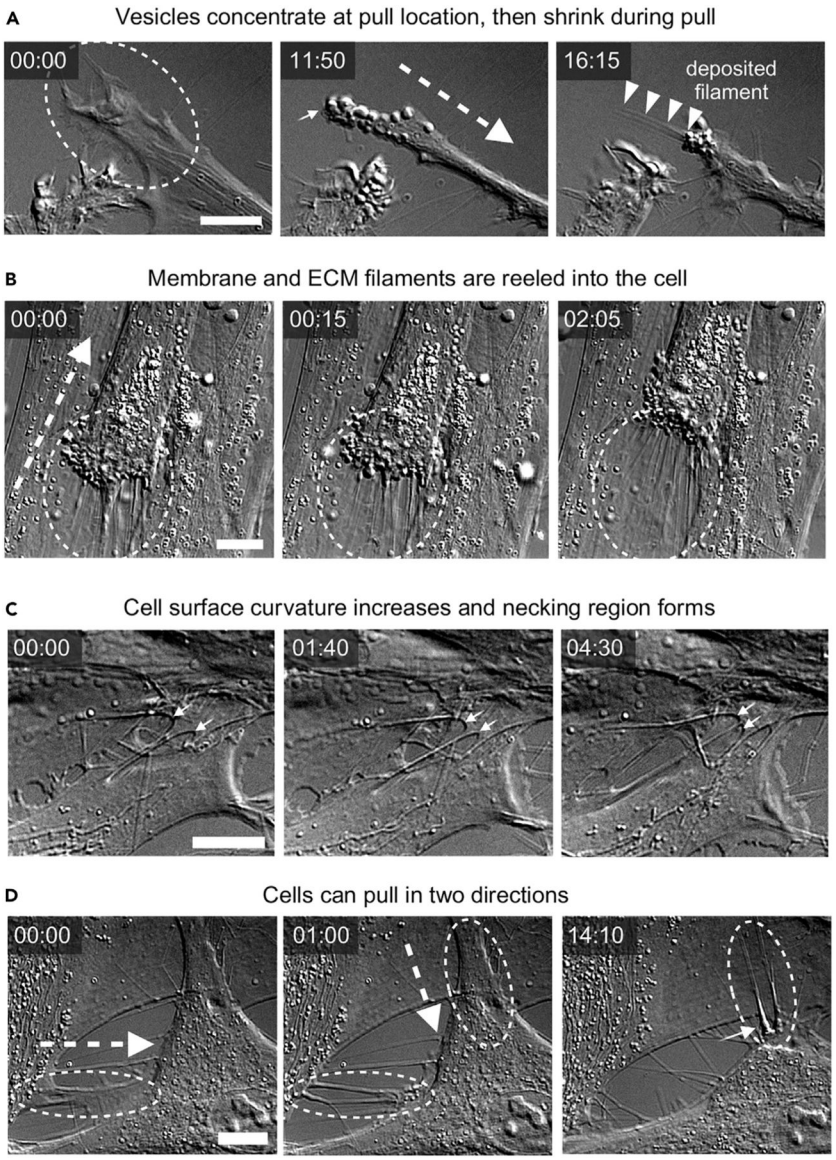

Figure 3. Notable observations during pulling events

(A) Bubble formation and dissipation. Long before the pulling event starts (left), no bubbles or vesicles are present. Just prior to the event (center), numerous vesicles appear and concentrate at the edges of the cell CP, as shown by the small arrow. During the pulling event, a filament is deposited directly onto the glass surface (indicated by small arrows), and the vesicles diminish and vanish.

(B) Filament reeling. During this pull, vesicles form and accumulate at the cell surface, particularly where filaments are forming. As vesicles deplete, new ones emerge in a rapid, bubbling manner. Concurrently, the cell appears to reel in the newly created filaments.

(C) Cell surface curvature. Prior to the pull, the filament's base curvature is relatively open, as indicated by small arrows. During the pull, the cell surface becomes more curved, evoking comparisons with the necking region described by Paten et al.[16]

(D) Multidirectional filament formation. Initially, the cell's left CP pulls inward, forming filaments. Subsequently, the cell's top CP engages to create additional filaments that are nearly perpendicular to the first set. These filaments are further pulled inward, resulting in a crumpled region at the filament's base (indicated by a small arrow).
Scale bars represent 10 μm. Large, dashed arrows indicate the direction of the pull. Time is presented in min:sec format. The images are snapshots taken at specified time points from Video S4.

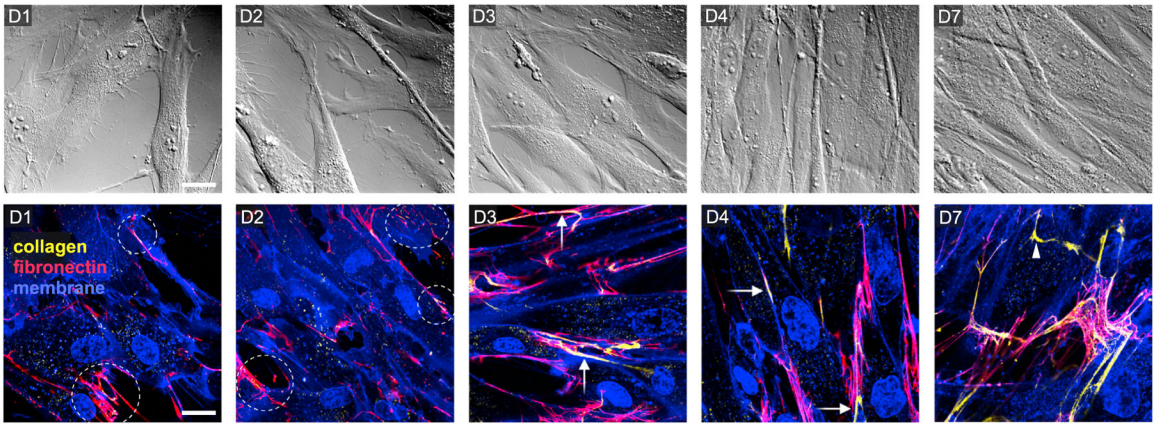

Figure 4. Progression of PHCF cell culture

Shown are representative DIC (top row) and confocal (bottom row) live-cell images captured on days 1–4 and day 7. Cells are stained for nucleus (blue), membrane (blue), FN (red), and collagen (yellow). During days 1–2, cells exhibit a flat morphology and are relatively sparse. FN is detectable on specific regions of the cell membrane, and punctate aggregates of exported collagen can be seen incorporated into some FN-associated membrane filaments (delineated by dashed circles). By days 3–4, the culture approaches confluence, with increased FN stretching between cells and a more linear rather than punctate appearance of collagen (indicated by arrows), suggesting the formation of collagen filaments. On day 7, some collagen filaments have disengaged from the FN membrane filaments (highlighted by a triangular arrow), evolving into independent structures that are anticipated to become “durable.” The scale bars represent 20 μm, and all images are presented at the same scale.

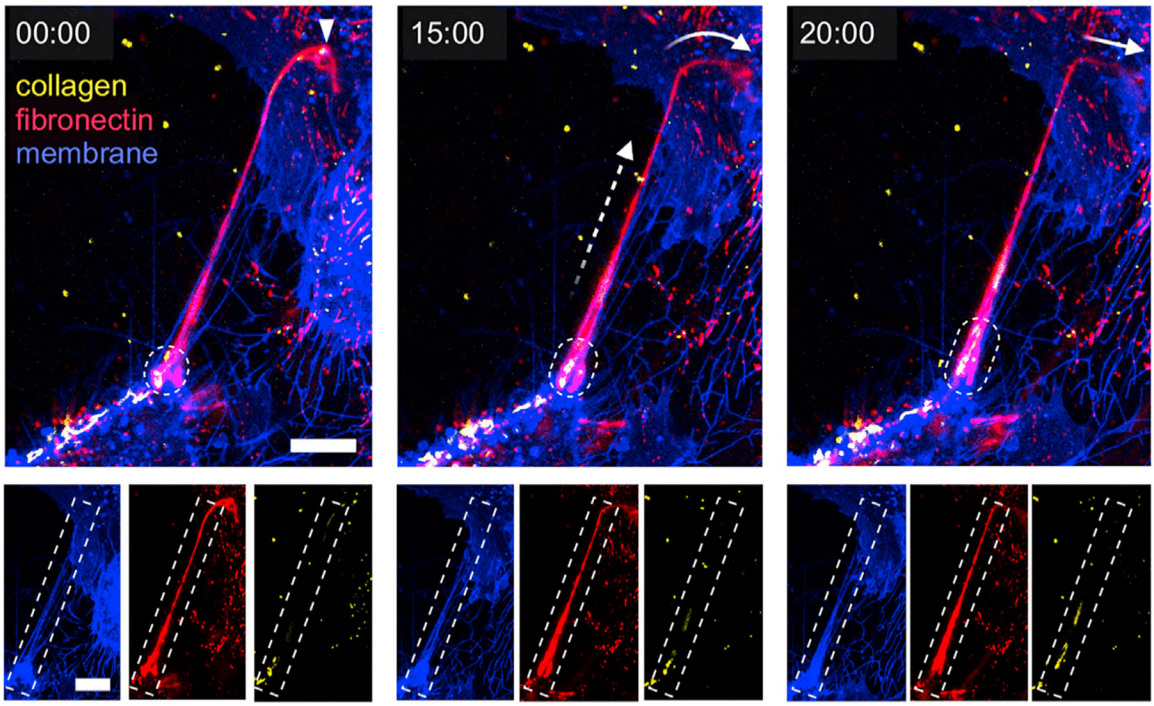

Figure 5. Colocalization and stretching of collagen and FN in membrane extensions

Shown is a thin membrane extension (blue) colocalized with exported collagen (yellow) and FN aggregates (red). The filament is stretched between two cells and is actively retracted by the upper cell, as indicated by the arrowhead. As the filament is pulled inward (depicted by the curved arrow), collagen localized at the filament's base (highlighted by dashed ellipses) stretches in the direction of the pull (represented by the dashed arrow), and the filament is reeled into the cell (straight arrow). Scale bars correspond to 10 μm, and time is presented in min:sec format. The bottom row offers isolated channel views at different time points to emphasize the distinct membrane, FN, and collagen compositions of the filament.

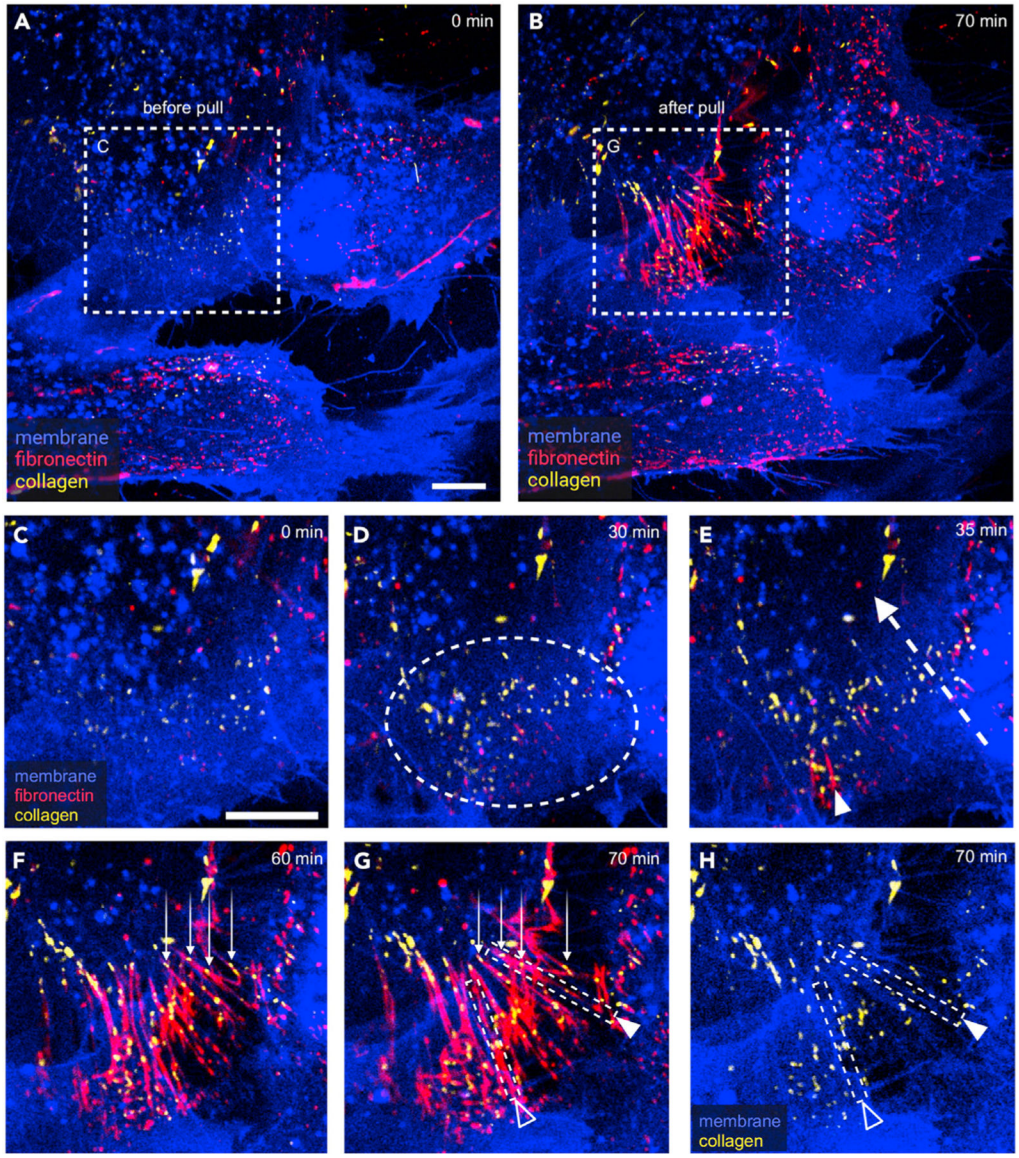

Figure 6. ECM structure formation induced by pulling events

Live-cell confocal microscopy of PHCF culture on day 1 shows cells stained for nucleus (blue), membrane (blue), FN (red), and collagen (yellow), with a focus between the cell and the glass substrate.

(A and B) Low-magnification images capture the cell environment before and after a slow cell-surface pulling event that leads to ECM formation.

(C–F) A high-magnification inset highlights the pulling event. Prior to the pull (C and D), punctate collagen and FN aggregates on the cell surface become more vibrant and numerous (circled). As the pulling commences (E), FN seems to “streak” (indicated by an arrowhead) in the direction of the pull (large dashed arrow), becoming brighter and starting to form a filamentous matrix (F). Collagen aggregates colocalize with FN (indicated by thin arrows) and elongate as the ECM stretches (F and G).

(G and H) A white arrowhead highlights an ECM filament containing a membrane core (small rectangle), while a hollow arrowhead points to an ECM filament lacking a membrane core (small rectangle). Subtraction of FN and membrane enhancement (H) reveals a network of membranous cell filaments that mostly colocalize with the newly formed ECM. Scale bars correspond to 10 μm. Images are snapshots taken at specific time points from Video S5.

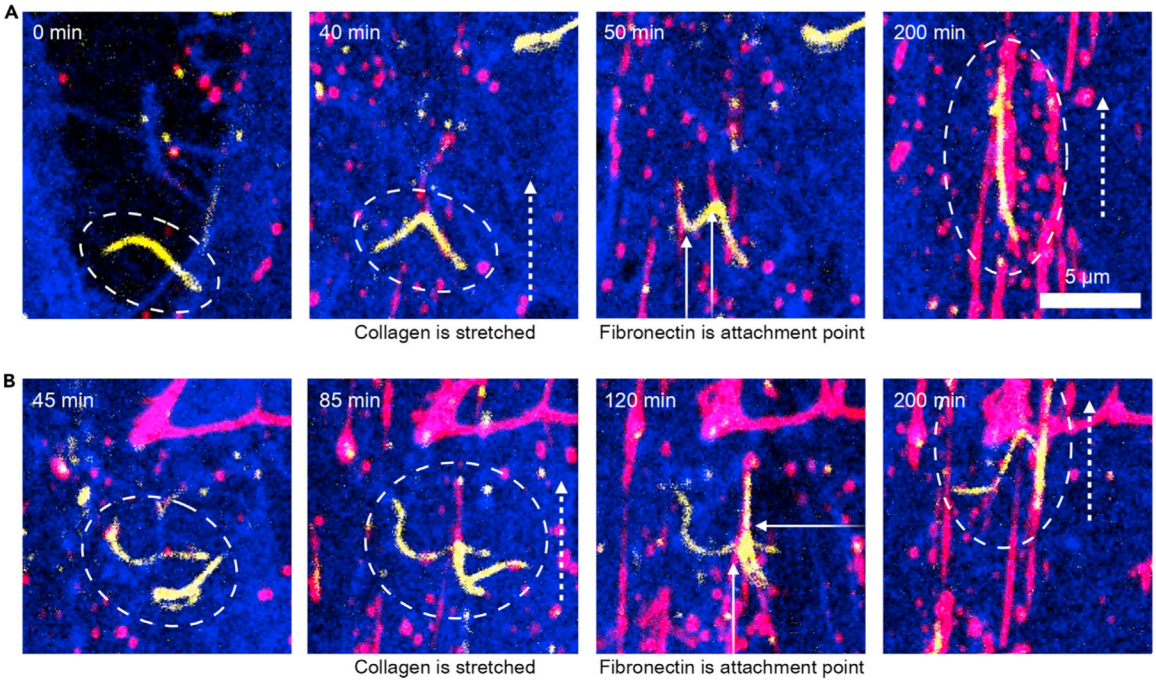

Figure 7. Collagen filament mutability and interaction with FN during pulling events

Live-cell confocal images show the PHCF culture stained for membrane (blue), FN (red), and collagen (yellow). Time-stamped snapshots are taken from Video S6 for reference.

(A and B) Existing short collagen filaments (shown in dashed circle) undergo modifications due to local pulling activity. Cells traverse and exert force (pull direction indicated by large dashed arrows) on these short collagen filaments, which subsequently bind to FN filaments (denoted by small arrows) and stretch alongside FN/membrane structures in the direction of the pull.

(A) A single collagen filament elongates longitudinally without visibly merging with other collagen filaments, possibly through the accretion of collagen molecules or aggregates and/or molecular reconfiguration.

(B) Two closely associated collagen filaments undergo stretching due to the same pulling event and binding to a shared FN filament. One of these collagen filaments appears to fold and laterally fuse with itself in the final frame captured.

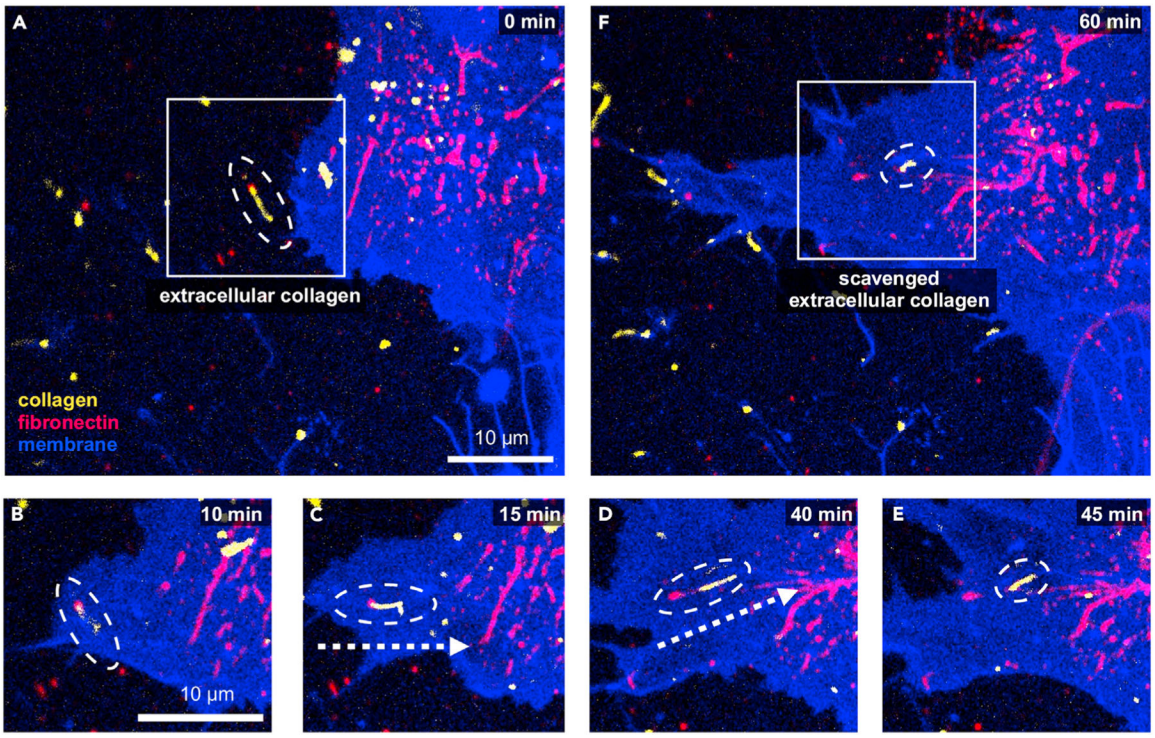

Figure 8. Dynamic collagen scavenging observed in PHCF culture

Live-cell confocal imaging shows a PHCF culture stained for membrane (blue), FN (red), and collagen (yellow). A cell moves over an extracellular collagen filament, outlined by a dashed ellipse (A). The cell binds (B and C) and subsequently stretches the collagen (D) in the direction of the dashed arrow. The tension on the collagen is released at the 45-min mark (E), ultimately leaving the collagen in a shortened, curled configuration and leading to the scavenging of this collagen (F). A small, punctate FN aggregate is initially bound to one end of the collagen filament (A–C). During stretching, the collagen detaches from this small FN aggregate on its left (D). Time-stamped snapshots are sourced from Video S7 for reference.

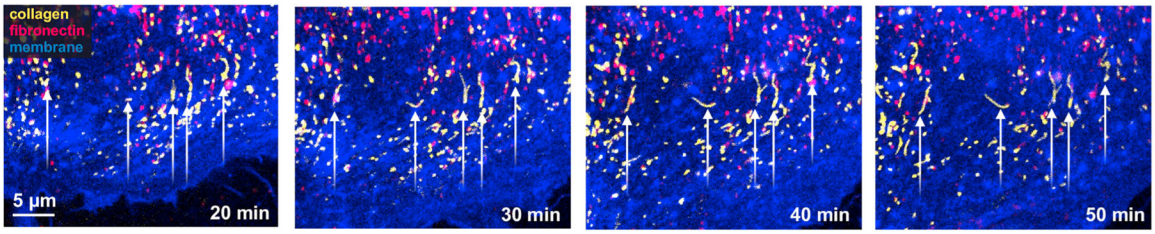

Figure 9. Formation of collagen "worms" in PHCF culture

Live-cell confocal images depict a PHCF culture stained for membrane (blue), FN (red), and collagen (yellow). In these settings, punctate collagen aggregates become trapped between the cell and the glass substrate, giving rise to short collagen filaments (indicated by arrows) without any associated pulling events. These resulting collagen filaments are typically short, measuring less than 5 μm in length (see Figure S5 for reference), and do not appear to be under tension. The images are time-stamped snapshots taken from Video S8 for context.

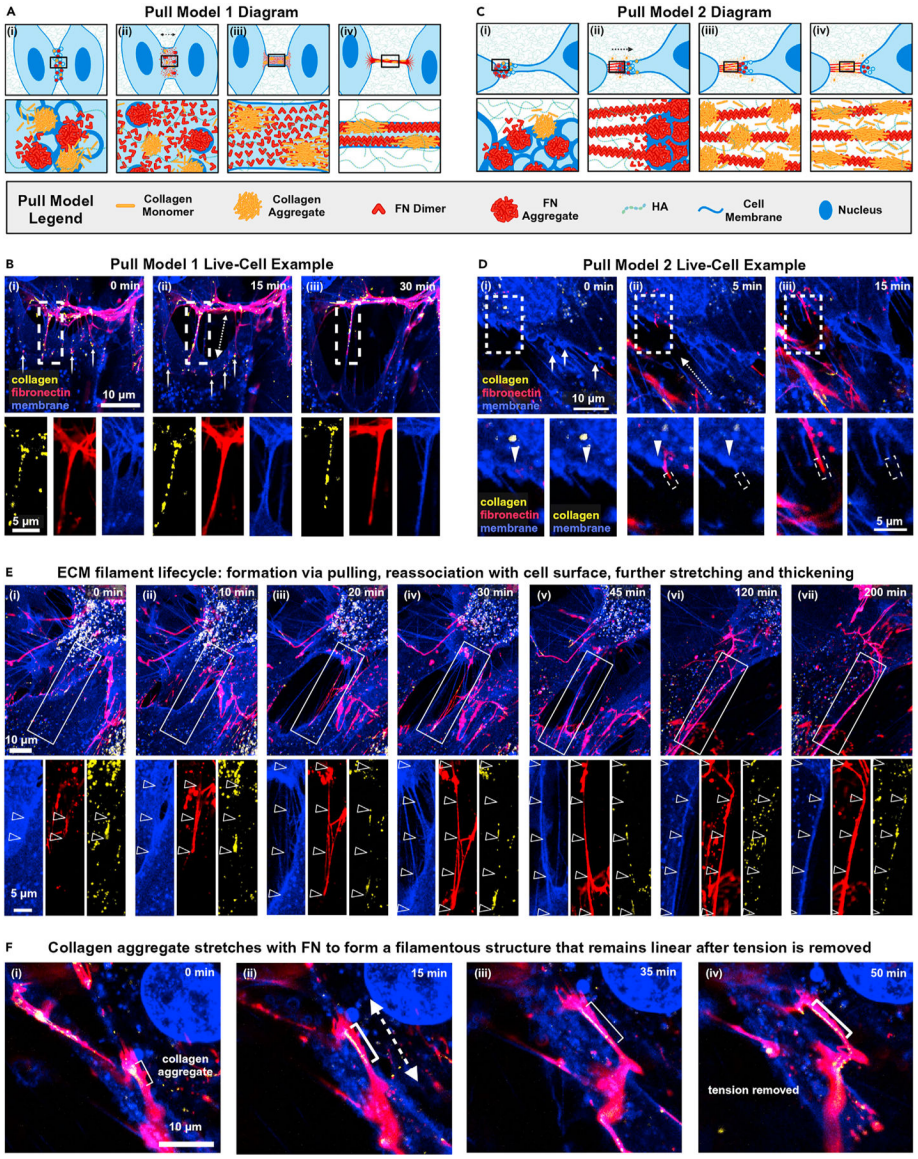

Figure 10. Mechanistic models for filament assembly in early, uncrowded environments

(A–E) Two proposed mechanistic models (A and C) along with corresponding live-cell confocal microscopy examples (B and D) for mechanically driven filament assembly in an early-stage, uncrowded cellular system. Time-lapse confocal images feature PHCFs stained for nucleus (blue), membrane (blue), FN (red), and collagen (yellow). Composite images are shown above each set of individual channels (B, D, and E), and the direction of cellular pulling is indicated by dashed arrows. Images used are snapshots from Videos S9 and S10. (A) Model 1 outlines a filament assembly process with a cellular membrane extension at its core. The sequence begins with two adjacent, bubbling cells releasing collagen and FN from their vesicles at the site of pulling (A, i). These molecules then adhere to the cell surface (A, ii) and become increasingly aligned as a membrane bridge forms between the separating cells (A, iii). As the bridge thins and elongates, FN molecules further align,

concentrate, extend, and polymerize to create filaments, while collagen aggregates and other ECM components also bind FN filaments and become aligned in the path of force (A, iv).
(B) Live-cell example supporting model 1. A filament comprising membrane, polymerized FN, and collagen aggregates is stretched between two adjacent cells (B, i). Additional FN and collagen aggregates are exported to the cell surface (small arrows). As the cells separate, the membrane core elongates and thins (B, ii and iii). FN appears brighter, thinner, and straighter, and collagen aggregates appear brighter, and more aligned.
(C) Model 2 proposes a filament formation mechanism without a cellular membrane at the core. This model begins with a single cell releasing collagen and FN from vesicles at the pulling site (C, i). These molecules accumulate due to external HA limiting their diffusion. The CP rapidly pulls, which exerts extensional strain on the surrounding molecules, causing the FIA of FN (C, ii). Collagen aggregates (and additional ECM biopolymers) can bind to the FN filaments (C, iii) and become stretched and aligned in the path of force (iv).
(D) Live-cell example supporting model 2. A bubbling cell releases vesicular content (small arrows; D, i). As the cell pulls (D, ii), an FN filament “streaks” out of a vesicle with no membrane extension at its core (vesicle indicated by arrowheads in the inset images; FN filament shown in dashed rectangle). The cell continues to pull, and the FN filament grows longer and thicker, with the end section only comprising FN (D, iii).
(E) An FN and collagen aggregate (E, i) is pulled and stretched into an FN filament with a cell membrane at its core (E, ii and iii; filament indicated by hollow arrows). The cell membrane core then dissipates and is no longer visible (E, iv), and then the FN filament associates with surrounding membrane filaments (E, v). Ultimately, the FN filament associates with the cell surface, is further stretched, and is thickened by associating with other FN on the cell surface (E, vi and vii).
(F) A small collagen aggregate (F, i) is stretched with FN into a filamentous structure (F, ii and iii) which remains linear even when tension is removed (F, iv) and then is later reorganized by the cells.